B. AREA OF REVIEW (AOR) AND CORRECTIVE ACTION (CA) PLAN
40 CFR 146.85

Vernon One CCS Site

Facility Name: Vernon One CCS Site

[redacted]

Facility Contact: Ronald T. Evans, tevans@capturepointllc.com
1101 Central Expy S, Suite 150, Allen, TX 75013
832-300-8225

Well Locations: Vernon Parish, Louisiana

[redacted]

Table of Contents

1.0 Computational Model Approach 7

1.1 Model Background 8
1.1.1 Static Model – Petrel 8
1.2.1 Dynamic Model – Reveal 9

1.2 Site Geology and Hydrogeology 10

1.3 Model Domain and Inputs 11

2.0 Model Input and Sources 13

2.1 Model Layering 15
2.1.1 Injection Zone 1 - [redacted] Formation 16
2.1.2 Injection Zone 2 - [redacted] 16
2.1.3 Injection Zone 3 - [redacted] 16

2.2 Rock Types 17

2.3 Porosity 18

2.4 Permeability 23

2.5 Rock Compressibility 24
2.5.1 Formation Compressibility 25
2.5.2 Formation Fluid Density, Compressibility and Viscosity 26

2.6 Constitutive Relationships 27

2.7 Boundary Conditions 28

2.8 Initial/Static Conditions 29

2.9 Operational Information 30

2.10 Fracture Pressure and Gradient 32

2.11 Characteristics of the CO_2 Stream 34
2.11.1 CO_2 Density and Compressibility 34
2.11.2 Viscosity 35
2.11.3 CO_2 and Formation Interactions 35
2.11.4 Solubility 35

3.0 Computational Modeling results 36

3.1 Predictions of Model Behaviour 36

3.2 Model Calibration and Validation 38

4.0 Model Results 39

4.1 Predicted Position of the CO_2 Plume 39
4.1.1 Ultimate Plume Extent 41
4.1.2 Plume Migration Post Closure 42

4.2 Predicted Position of the Presure Front 43

4.2.1 Net Pressure Build-up 43
4.2.2 Pressure Stabilization Post Shut-in 43

5.0 Area of Review 44

5.1 Critical Pressure Calculations 44

5.2 AoR Delineations 44

6.0 Corrective Action Plan 46

6.1 Tabulation of Wells within the AoR 46
6.1.1 Wells within the Area of Review Data Bases and Search Protocol 48
6.1.2 Well Evaluation 49
6.1.3 Wells Penetrating the Confining Zone 50

6.2 Plan for Site Access 50

6.3 Corrective Action Schedule 50
6.3.2 Well 1 – Bentley Lumber Co. No 6 – Corrective Action Plan 51
6.3.4 Well 2 – Pardee No 2 – Corrective Action Plan 56
6.3.6 Well 3 – William Burton No 2 – Corrective Action Plan 60
6.3.7 Well 4 – Crosby Chemicals No 1 – Corrective Action Plan 64
6.3.8 Well 8 – Indigo 25 H – Corrective Action Plan 65

7.0 Re-evaluation Schedule and Criteria 66
7.1 AoR Re-evaluation Cycle 66
7.2 Triggers for AoR Reevaluations Prior to the Next Scheduled Reevaluation 66

8.0 References: 68

List of Tables

Table 1: Modeled Considerations 7
Table 2: LAS files used in the Static Model 8
Table 3: Model domain information. 12
Table 4 – Available logs for analysis 13
Table 5 – Log Type Identification 13
Table 6 – Available core data for analysis 14
Table 7: Model Layering 15
Table 8: Dynamic Model Layer Thickness 16
Table 9 - Total Porosity Measurements from Available Core 19
Table 10 – Minimum Effective Shale Porosity in Gulf Coast Environments 20
Table 11: Porosity inputs into the Model by layer: 22
Table 12: Porosity-Permeability Transforms used in the Reveal Model. 24
Table 13: Compressibility for the Injection Zones 25
Table 14: Initial Viscosity at Nominal Conditions 27
Table 15: Relative Permeabilities and Saturation Factor inputs into Reveal 28
Table 16: Initial conditions for the [redacted] *at well V1- CCS #7.* 29
Table 17: Initial conditions for the [redacted] *at well V1- CCS #8* 29
Table 18: Initial conditions for the [redacted] *at well V1- CCS #3* 30
Table 19: Operating details for Injection Zone 1 - [redacted] 30
Table 20: Operating details for Injection Zone 2 – [redacted] 31
Table 21: Operating details for Injection Zone 3 – [redacted] 31
Table 22: Calculated Fracture Pressure 33
Table 23: Injection pressure details – [redacted] * 33
Table 24: Injection pressure details – [redacted] * 33
Table 25: Injection pressure details – [redacted] * 34
Table 26: Property inputs for CO_2 34
Table 27: Injection Data for Wells complete in Injection Zone 1 - [redacted] * 37
Table 28: Injection Data for Wells complete in Injection Zone 2 - [redacted] * 37
Table 30: Absolute Modeled Plume Extent at 70-years, 50 years post closure – Top Layer 40
Table 31: Absolute Modeled Plume Extent at 70-years – Bottom Layer 41
Table 32: Plume Migration Post Closure for Injection Zone 1 – [redacted] 42
Table 33: Plume Migration Post Closure for Injection Zone 2 – [redacted] 42
Table 35. List of wells within the AoR 47
Table 36 – Bentley Lumber Co. No 6 – Proposed Cementing Details 55
Table 37 – Pardee No 2 – Proposed Cementing Details 59
Table 38 – William Burton No 2 – Proposed Cementing Details 63

List of Figures

1A. AoR and Plume Delineation Map

1B. Well Location Map

2A. Well Cross Section Along Strike

2B. Well Cross Section Along Dip

3A. Well Log of the [redacted]

3B. Well Log of the [redacted]

3C. Well Log of the [redacted]

4. Geographic Extent of the Static Model

5. 3D Skeleton Grid of the Static Model

6. Model Cross Section Along Strike

7. Model Cross Section Along Dip

8. Method 2 for Rock Selection

9. Porosity Comparison – Hanna Well

10. Formation Fluid Viscosity

11. Formation Fluid Density

12. Density and Viscosity as a Function of Pressure and Temperature – [redacted]

13. Density and Viscosity as a Function of Pressure and Temperature – [redacted]

14. Density and Viscosity as a Function of Pressure and Temperature – [redacted]

15. Calculated Fracture Gradient – [redacted]

16. Calculated Fracture Gradient – [redacted]

17. Calculated Fracture Gradient – [redacted]

18. CO_2 Density – [redacted]

19. CO_2 Density – [redacted]

20. CO_2 Density – [redacted]

21. Plume Density at Leading Edge of Plume – [redacted]

22. Plume Density at Leading Edge of Plume – [redacted]

23. Plume Density at Leading Edge of Plume – [redacted]

24. Super Critical CO_2 Viscosity Graph – [redacted]

25. Super Critical CO_2 Viscosity Graph – [redacted]

26. Super Critical CO_2 Viscosity Graph – [redacted]

27. Modeled Plume Extent for the Top Layer – [redacted]
28. Modeled Plume Extent for the Top Layer – [redacted]
29. Modeled Plume Extent for the Top Layer – [redacted]
30. Modeled Plume Extent for the Bottom Layer – [redacted]
31. Modeled Plume Extent for the Bottom Layer – [redacted]
32. Modeled Plume Extent for the Bottom Layer – [redacted]
33. Pressure Equilibrium Initial and Final Pressure Upper Layer – [redacted]
34. Pressure Equilibrium Initial and Final Pressure Upper Layer – [redacted]
35. Pressure Equilibrium Initial and Final Pressure Upper Layer – [redacted]
36. Pressure Equilibrium Initial and Final Pressure Bottom Layer – [redacted]
37. Pressure Equilibrium Initial and Final Pressure Bottom Layer – [redacted]
38. Pressure Equilibrium Initial and Final Pressure Bottom Layer – [redacted]
39. Delineation of AoR Boundary
40. Bentley Lumber Co. No 6 Existing Plugs
41. Bentley Lumber Co. No 6 Proposed Plugging
42. Pardee No 2 Existing Plugs
43. Pardee No 2 Proposed Plugging
44. William Burton No 2 Existing Plugs
45. William Burton No 2 Proposed Plugging
46. Crosby Chemicals No 1 Existing Plugs
47. Indigo 25 H Existing Plugs

List of Appendices

Appendix 1 Reveal Simulation Software User Manual
Appendix 2 Structure Horizons for Model
Appendix 3.1 Workflow for Porosity and Porosity Maps
Appendix 3.2 Workflow for Permeability and Permeability Maps
Appendix 4 Pressure and Rate Time Series Plots
Appendix 5.1 Plume Time Series Plots – [redacted]
Appendix 5.2 Plume Time Series Plots – [redacted]
Appendix 5.3 Plume Time Series Plots – [redacted]
Appendix 6.1 CO_2 Plume Saturation Movement – [redacted]

Appendix 6.2 CO_2 Plume Saturation Movement – [redacted]
Appendix 6.3 CO_2 Plume Saturation Movement – [redacted]
Appendix 7.1 Pressure Front Contours – [redacted]
Appendix 7.2 Pressure Front Contours – [redacted]
Appendix 7.3 Pressure Front Contours – [redacted]
Appendix 8.1 Pressure Buildup – [redacted]
Appendix 8.2 Pressure Buildup – [redacted]
Appendix 8.3 Pressure Buildup – [redacted]
Appendix 9 Corrective Action Well Sundries

1.0 COMPUTATIONAL MODEL APPROACH

The modeling is intended to present a conservative estimate of pressure build-up and plume extent over the injection and post injection life of the project. The data used in the model is derived from regional data, and from wells in near proximity to the project site. Until information is obtained from site specific wells, input data is used to create a conservative estimate (larger) of pressure build-up and plume extent. This model represents a preliminary scenario for computational modeling at the Vernon One CCS Site and will be updated to a final simulation scenario following acquisition of additional data from a planned site characterization well.

There are various physical and chemical processes that determine the efficiency and viability of CO_2 sequestration. **Table 1** contains some of the modeled considerations. This study primarily considers the effects of stratigraphic trapping by the primary confining unit and to some degree capillary pressure trapping. Relative permeability and capillary pressure curves used in the model are conservative. In addition, hysteresis (imbibition) trapping has not been modeled.

Table 1: Modeled Considerations

Process	Modeled
Stratigraphic trapping (Primary Confining Unit)	Yes
Structural Trapping	N/A
Hydrodynamic Trapping	No
Residual Gas Trapping	No
Capillary Trapping	Capillary Pressure
CO_2 solubility trapping with the in-situ formation water	No
Mineralogical transformation	No

The model was first built using geological parameters to build a static model within Petrel for all three targeted injection zones. The static model was then input exported in ASCII format for import into Reveal for dynamic simulation. It is through dynamic simulation that pressure and plume movement for each of the three targeted injection zones can be predicted and quantified. Where available, assumptions and inputs in the models have been validated for site specific conditions. At present, no historical data exists to calibrate models, but will be developed as the project operates.

Results from the computational models are used to establish an Area of Review (AoR). The AoR is defined as the area surrounding the sequestration project where the underground sources of drinking water (USDWs) may be endangered by injection operations. For the Vernon One CCS site, this area encompasses the maximum lateral extent of the CO_2 plume (modeled) and the resulting critical pressure front (cone of influence) preceding the plume. The shallowest of the three targeted injection zones ([redacted]) produced the largest plume and cone of influence and was thereby selected to define the AoR for the site. The AoR for each injection zone will be updated and provided following the collection of site-specific information collected from the drilling of a stratigraphic test well and the injection wells. For the purpose of this initial modeling effort only the largest ([redacted]) AoR is provided (**Figure 1A**). Note that

groundwater monitoring wells are noted as "GWM" and in-zone monitoring wells are noted as "IZM" on the map.

The following discussions highlight each model and their impact for developing the Area of Review and Corrective Action Plan for the CapturePoint Solutions, Vernon One CCS Site.

1.1 MODEL BACKGROUND

1.1.1 Static Model – Petrel

Schlumberger's Petrel software was used to generate a static geocellular model for use in Petroleum Experts dynamic simulation software (Reveal). Petrel was developed in Norway in 1989 by Technoguide, and later acquired by Schlumberger in 2002. This software was designed to perform reservoir modeling in 3D, incorporating offset well log/core data, seismic data, and to be linked with commercially available reservoir simulators.

Petrel was selected for this project because of its easy-to-follow workflow design, and because it is one of if not the industry leader for static geocellular modeling. It has been designed and used worldwide for reservoir evaluation and development.

Model construction begins with the definition of the model objective. For the Vernon One CCS Class VI Sequestration project, the model objective was to:

- Generate a 3D realization of the subsurface within a defined area that incorporates each injection interval and each impermeable overlying rock layer.
- Populate the model with key rock properties using the existing dataset and stochastic distribution. For this project the dataset allowed for the calculation of Porosity, and Permeability and an estimation of the expected net sand.
- The model is then evaluated through dynamic simulation using Reveal, to study the impact of the distributed critical properties controlling the ability of the rock to allow injection, measure the pressure response of the rock to the injected CO_2, prediction of the storage capacity of the selected injection interval, and to track the expected movement of the CO_2 plume under those injection interval conditions.

The identification of available data is a critical first step in model construction. This core data set often includes wells, well logs, core*, rock data*, fluid data* and seismic*. For projects investigating the permanent storage of CO_2 highly developed hydrocarbon prone stratigraphy is not an ideal setting. Most often the data described above is found in areas where extensive oil and gas exploration has taken place. For the generation of the static geological model project, the primary data set included only wells and logs. LAS files were located and or generated (See the location of these wells on the map in **Figure 1B**) of the 21 wells, 7 have sonic, density and neutron curves enabling the calculation of Total Porosity curves (**Table 2**).

Table 2: LAS files used in the Static Model

WELL NAME	UWI	STATUS	LOGS IN PETREL
AJ HODGES	17115200250000	P&A	DT, RES, ILD, LL8, SFL, SPR, CILD, MCAL

WELL NAME	UWI	STATUS	LOGS IN PETREL
ALMCO NO 1	17069203480000	P&A	DT, GRR, ILD, ILM, SFLU, NPHI, RHOB, DCOR, SPR, DCAL, PE
BENTLEY #A-1	17115200080000	P&A	GR, RESD, RESM, RESS, NEUT, DEN, SONIC, SP, CALI, PHI-T, VSH, NET SAND
BLM 26-5	17079201940000	P&A	RASTER RES
DOWDEN BRANCH	17069202210000	P&A	GRR, ILD, ILM, SFLU, SPR
INTERNATIONAL PAPER COMPANY #1	17079203510000	P&A	GR, RESD, RESM, RESS, SONIC, SP, CALI, PHI-T, VSH, NET SAND
J. W. HANNA JR #1	17079203750000	P&A	GR, RESD, RESM, RESS, NEUT, DEN, SONIC, SP, CALI, PHI-T, VSH, NET SAND
JOHN A. DUNNAM #1	17079202270000	P&A	RESD, RESM, SP, VSH, NET SAND
JOHN E. ERVINE #1	17079007010000	P&A	RESD, RESM, RESS, SP, VSH, NET SAND
MARTIN LUMBER CO 1	17079203840000	P&A	DT, GR, RTLG, SNLG, SPR, CALS
MARVIN DEVLOPEMENT CO	17115200050000	P&A	GR, ILD, ASN, SPR, CILD
SHELL JA BENTLEY LUMBER CO 1	17079203650000	P&A	GR, RESD, RESM, NEUT, SONIC, SP, CALI, PHI-T, VSH, NET SAND
SOCONY MOBIL BENTLEY #1	17079000150000	P&A	GR, RESD, RESM, RESS, SONIC, SP, CALI, PHI-T, VSH, NET SAND
TEXACO JA BENTLEY LUMBER CO INC 1	17079201110000	P&A	GR, RESD, RESM, RESS, SONIC, SP, CALI, PHI-T, VSH, NET SAND
USA 13-13	17079201880000	P&A	RESD, RESM, SP, VSH, NET SAND
USA 6-2	17079202130000	P&A	RESD, RESM, SP, VSH, NET SAND
USA LROC 34 #1	17079204390000	P&A	GR, RESD, RESM, RESS, NEUT, DEN, SONIC, SP, CALI, PHI-T, VSH, NET SAND, PE

Regional core data was located using the Shreveport Online Database. The manner in which this data was utilized to determine a porosity-permeability relationship for this project is detailed in **Section 3.0** of this technical report.

1.2.1 Dynamic Model – Reveal

Petroleum Experts' Reveal software has been selected for use in this study given its specialized modeling capabilities. Reveal is used throughout the energy and environmental industries by thousands of users. The software is fully thermodynamic and includes compositional EOS modeling of the fluids. Reveal provides several solvers (IMPES, Fully Implicit) and handles a variety of gridding scenarios (Cartesian, Corner Point, Curve-Linear, Radial and Core). The software provides the ability to model advective, diffuse and dispersive flow. In addition, Reveal incorporates the PHREEQC database to calculate ionic and chemical reaction processes. Geo-mechanical modeling of the "cap rock integrity" and/or hydraulic fracturing is also available in the software. **Appendix 1** contains the User manual for the Revel Software.

This study models the mass injection and advective flow of super critical CO_2 into an initially fully saline-water saturated reservoir using the finite difference method. The models include the effect of buoyant forces (gravitational effects) created by the density contrast between the CO_2 injectate and the in-situ water. Temperature effects, caused by injection of cooler fluid into the reservoir, and depth related in-situ temperature variations, are also modeled.

CO_2 density is estimated using Reveal's implementation of the Peng-Robinson (1978) equation of state. Reveal solves the equation by taking the pressure, temperature, and the starting composition of a grid cell. It then provides the composition of each of the two possible phases in which the fluid might exist, either a gaseous and/or an liquid phase for that cell. The mole density (number of moles per unit volume of the phase) is also calculated. The Lorenz, Bray Clark method is used to estimate CO_2 viscosity.

Petroleum Experts provides an internal method to estimate the density and viscosity of aqueous phases. These methods are presented in **Appendix 1**. Although not implemented for the modeling in this submission, Reveal also provides an estimate of water density created by the solution of the injected CO_2.

Regarding the finite difference method, there are many publications that offer very detailed explanations of how this method is implemented. Documentation provided by Petroleum Experts specific to Reveal is included in **Appendix 1** of this study.

1.2 SITE GEOLOGY AND HYDROGEOLOGY

Demonstration of security for injection includes a geologic containment demonstration and the absence of vertically transmissive faults that could form breaches of the containment system. The Vernon One CCS site is located in an area of no major geological structural impacts (*i.e.* faults, uplifts, domes). The reservoir sands are composed of a series of stacked, alternating sands and shale beds, with minor lignite layers. The layering is textbook "layer cake" in the sense that the geologic beds exhibit minor dipping to the south-southwest. The Eocene-aged formations have not produced oil or gas within the targeted site. As a result, there are few artificial penetrations that could act as conduits for fluid migration.

The reservoir units are overlain by three massive (and regionally extensive) impermeable shale formations ([redacted]). These layers provide a competent primary and secondary confining unit for the injection reservoir unit to prevent vertical migration of CO_2 out of the targeted intervals. A regionally extensive lower confining unit ([redacted]) is also well documented throughout Louisiana.

Figures 2A and 2B are strike and dip cross section view of the model highlighting the Injection and Confining Intervals within the static model. There are three injection zones modeled:

[redacted]

There are four confining/impermeable zones modeled as well:

[redacted]

These intervals are identified in the more detailed well-section view presented in **Figures 3a ([redacted]), 3b ([redacted]) and 3c ([redacted])** using the [redacted].

Injection Zone 1 is the [redacted] Formation, which is bound by the [redacted] (upper confining zone) and the [redacted] (lower confining zone) shale layers. The [redacted] is composed of mostly very fine to medium unconsolidated quartz that is ferruginous in places to form limonitic orthoquartzite ledges. The deposition environment is primarily beach and fluvial, and the formation contains subordinate beds of sandy clay and clay.

The [redacted] is divided into the [redacted], and [redacted] with the semi-regional [redacted] as the divide between the [redacted]. Injection Zone 2 is the [redacted], which is bounded by the [redacted] (upper confining zone) and the [redacted] (lower confining zone). The [redacted] is transgressive with locally regressive delta lobes deposited during a global rise in sea level. An increase in the carbonate content and glauconite content is predominant in the [redacted] sediments which suggests an increase in marine deposition as compared to [redacted].

Injection Zone 3 is the [redacted], which is bounded by the [redacted]" (upper confining zone) and the [redacted] (lower confining zone). The [redacted] is deposited in fluvial and deltaic environments. The strata are comprised of interbedded lenticular sands, mud, and lignite.

All injection zones are located at least 2,500 feet below the lowermost aquifer that meets the criteria for being a USDW (less than 10,000 mg/l total dissolves solids content).

A more detailed description of the Injection Zones can be found in **Section 2.0** – Site Characterization in the "*Project Information Narrative*", submitted in **Module A**.

1.3 MODEL DOMAIN AND INPUTS

The static model covers an area of 227,000 by 166,000 feet (~42.9 x 31.4 miles) or approximately 1,347 square miles, to account for a potential injection project to the east of the Vernon One CCS site in Vernon Parish. It is predominantly confined to Rapides and Vernon Parishes in Louisiana. With the northernmost extent of the model reaching into Grant and Natchitoches Parishes (**Figure 4**). These dimensions are needed to model the simultaneous injection and pressure interference from two proposed sites.

- The Vernon site, which is the subject of this permit application,
- The Rapides Parish site, which has applied for a Class VI permit, located approximately 18 miles east of the Vernon location.

Although this model considers potential injection in Rapides Parish site, the focus of this report is on the injection operations for the Vernon One CCS sites. Potential impacts from the Rapides site are considered.

Figure 5 shows the skeleton grid in 3D and the model domain information is summarized in **Table 3**.

Table 3: Model domain information.

Coordinate System	SPCS27_1701: NAD27 Louisiana State Planes, Northern Zone, US Foot		
Horizontal Datum	Mean Sea Level (MSL)		
Coordinate System Units	Feet-US		
Zone	Louisiana State Planes North		
FIPSZONE	1701	**ADSZONE**	4026
Coordinate of X min	1758755.79	**Coordinate of X max**	1985755.79
Coordinate of Y min	149028.94	**Coordinate of Y max**	315028.94
Minimum Depth (Z)-TVDSS	-780.206	**Maximum Depth (Z)-TVDSS**	-11074.4

The corner point grid created in Petrel was exported in "Eclipse ASCII format" and imported into Reveal dynamic simulation software. The grid has 454 cells in the X direction, 332 cells in the Y direction, and 16 total layers. Each cell block has uniform x-y dimensions of 500 x 500 feet respectively. Cell block height varies depending on the distance between the upper and lower confining zones for each injection interval.

This excerpt, from the Reveal Users guide, describes the implementation of the corner point grid within the software.

*"Corner point (full) - in this scheme each block has 8 independent coordinates, giving (2*NX) * (2*NY) * (2*NZ) coordinates in total. These are entered as X, Y and Z coordinates for each layer, with (2*NX) * (2*NY) entries per layer for each spatial direction. Each block is considered in turn and its two corner point coordinates are entered before the next block data is entered."*

The origin (cell block 1,1,1) in Reveal is in the upper left (Northwest) corner of the grid. Layer 1 is the shallowest layer. Depth increases with each subsequent layer number. Layer dimensions are measured in feet (ft) and vertical distance is measured in True Vertical Depth (TVD) relative to sea level (tvd-ss).

The upper left corner of the origin cell (1,1,1) corresponds to geospatial coordinates of 1758755.791 easting, 315028.938 northing using NAD27 North - Louisiana State Plane coordinates. The grid extends horizontally 227,000 ft (39.4 mi) and 166,000 ft vertically. The geospatial coordinates of the southeast corner of the grid, cell (454,332,1), are 1985755.791 easting and 149028.938 northing.

2.0 MODEL INPUT AND SOURCES

Multiple sets of data were used to evaluate and determine parameter inputs in the models for the Vernon One CCS Site. Data sets included available offset well logs, that are of sufficient quality, limited local core representative of the [redacted], regional core from northeast Rapides Parish, and published literature sources. Conservative assumptions were made when data was insufficient, and the data limitation will be resolved with the drilling of a stratigraphic test well and incorporating the results into the model iteration.

Nine analogs were analyzed due to the quality of the log and proximity to the injection site. These logs are listed in **Table 4** and their locations are shown on **Figure 1**. **Table 5** identifies the types of logs and their measurement of the formations.

Table 4 – Available logs for analysis

API Number	Well Name	Lithology Logs	Porosity Logs	S_{w*}
17079000150000	Bentley LBR CO No A 1	GR, SP	DTC	RES
17079203510000	International Paper Co #1	GR, SP	DTC	RES
17079202270000	J A Dunnam No 1	SP, RES	N/A	N/A
17079203750000	J W Hanna Jr #1	GR, SP	DEN, NEU, DTC	RES
17079007010000	John E Ervine #1	SP, RES	N/A	N/A
17079204390000	USA – LROC 34#1	GR, SP	DEN, NEU, DTC	RES
17079201880000	USA 13-13 #1	SP, RES	N/A	N/A
17079202130000	USA 6-2	SP, RES	N/A	N/A
17079204140000	William E Cooper Jr #1	SP, RES	DEN, NEU, DTC	RES

**Water Saturation*

Table 5 – Log Type Identification

LOG Acronym	Log Type	Unit of Measurement	Log Measurement
GR	Gamma Ray	API	Total natural gamma radiation emanating from a formation.
SP	Spontaneous Potential	Millivolts (mV)	Natural spontaneous current flow between the borehole and surface in absence of artificially applied current.
RES	Resistivity	Ohms-m	Measures a formations electrical resistivity using and an electric current.
DTC	Acoustic/Sonic	Microseconds/ft	Measurement of compressional (primary) wave transit times through a formation.

LOG Acronym	Log Type	Unit of Measurement	Log Measurement
DEN	Density	Rhob	Density of the formation by using gamma rays into a formation and measuring the scatter back to tool
NEU	Neutron	p.u.	Measurement of porosity using the input of neutrons into the formation and measuring the reduction in energy due the hydrogen.

Local and regional core data was available for evaluation for the [redacted] Injection Zones (**Table 6**). Regional core samples are representative of the formations slightly updip from Vernon Parish. A combination of whole core plugs and rotary sidewall core measurements were obtained from publicly accessible repositories, the source of the measurements was identified in individual laboratory reports.

Table 6 – Available core data for analysis

[redacted]

Note: *Core data was not available for the* [redacted] *Formation.*

Petrophysical properties such as grain density, porosity and permeability were calibrated using core. The following sections details the model input into the static and dynamic model.

2.1 MODEL LAYERING

Static model construction begins with the generation of the model framework. For the Vernon One CCS site, no faults were identified on available 2D seismic data or on commercially available structure maps for study area. Therefore, model construction began with the correlation of [redacted] key stratigraphic intervals: [redacted]. Of the nine stratigraphic intervals, [redacted]) were converted to structured surfaces in Petrel using the well tops as the foundation. These Structured Surfaces (or Horizons), and the wells used to create them are shown in **Appendix 2**. These surfaces were then used as inputs into the model construction workflow, utilizing the "make simple grid" function in Petrel. These seven Horizons compose the major framework of the model. A breakdown of the horizons is provided in **Table 7**.

Table 7: Model Layering

Formation	Model Purpose of the Formations/Horizons	Horizon Number	Average Gross Thickness Between Horizons	Static Model Layers	Average Gross Layer Thickness at the Wells (feet)
[redacted]	Impermeable Layer	1	292	1	292
[redacted]	Top of [redacted] Injection Interval	2	526.7	2, 3, 4	176
[redacted]	Impermeable Layer	3	363	5	363
[redacted]	Top of [redacted] Injection Interval	4	1,342	7, 8, 9, 10	268
[redacted]	Base of [redacted] Injection Interval-Top of Impermeable Layer	5	97	11	97
[redacted]	Top of [redacted] Injection Interval	6	2,323	12, 13, 14, 15, 16	465
[redacted]	Base of the Model Horizon	7	--	--	--

Due to the thickness of the proposed injection intervals, further subdivision of these intervals was required. Therefore, additional layering was added to the [redacted] injection intervals. These layers were added into the model using proportional layering between the top and base horizons. The layers are summarized in **Table 7**. An intersection window of these additional layers can be seen in **Figures 6 (along strike) and 7 (along dip)**.

Layering derived from the static model is transformed for use in three independent dynamic models for of each of the proposed injection intervals. Each formation had an average gross layer thickness (in feet), that was then equally divided into the modeled layers.

2.1.1 Injection Zone 1 - [redacted]

The overlying [redacted] confining zone is layer 1 in the Petrel Static model. The Cane River lower confining zone is layer 5 in the Petrel Static model.

The [redacted], upper confining zone, is assumed to mitigate all vertical migration of CO_2 while the [redacted] zone (confining unit), is assumed to prevent vertical flow below the base of the [redacted] formation. Given the assumptions regarding the confining zones, only layers 2, 3, and 4 are used in the dynamic model to represent the [redacted]. A total average layer thickness of 513 feet was used for the formation, with each of the three model layers (2, 3, and 4) being assigned an equal proportion. Average layer thickness per layer is 171 feet. The confining layers have not been specifically modeled. Layers 2, 3, and 4 have been re-numbered as layers 1, 2 and 3 to conform to Reveal's grid coordinates.

2.1.2 Injection Zone 2 - [redacted]

The overlying Cane River confining zone is layer 5 in the Petrel Static model. The [redacted] lower confining zone is layer 11 in the Petrel Static model.

The Cane River, upper confining zone, is assumed to mitigate all vertical migration of CO_2 while the [redacted] (confining unit), is assumed to prevent vertical flow below the base of the [redacted] Given the assumptions regarding the confining zones, only layers 6, 7,8, 9, and 10 are used in the dynamic model to represent the [redacted]. The [redacted] has an average thickness of 1,314 feet, with each of the five model layers (6, 7, 8, 9 and 10) being assigned equal proportion which equates to average thickness of 263 feet each. The confining layers have not been specifically modeled. Petrel layers 6 through 10 are re-numbered as layers 1 to 5 to conform to Reveal's grid coordinates.

2.1.3 Injection Zone 3 - [redacted]

The overlying [redacted] confining zone is layer 11 in the Petrel Static model. The [redacted] lower confining zone is the terminal boundary layer in the Petrel Static model.

The [redacted] upper confining zone, is assumed to mitigate all vertical migration of CO_2 while the [redacted] (confining unit), is assumed to prevent vertical flow below the base of the [redacted] formation. Given the assumptions regarding the confining zones, only layers 12, 13,14, 15 and 16 are used in the dynamic model. The [redacted] has average thickness of 2,246 feet, with each of the five model layers (12, 13, 14, 15 and 16) being assigned equal proportion which equates to average thickness of 449 feet each. The confining layers have not been specifically modeled. Petrel layers 12 through 16 are re-numbered as layers 1 to 5 to conform to Reveal's grid coordinates.

Table 8: Dynamic Model Layer Thickness

	h (min) ft	h (max) ft	h (avg) ft	Num Layers	h (avg) ft
[redacted]	313	681	513	3	171
[redacted]	943	1536	1314	5	263
[redacted]	1340	3062	2246	5	449

2.2 ROCK TYPES

Potential injection or seal units are first identified using a shale volume estimate (Vsh). The Vsh estimate effectively normalizes a combination of electrical logs with responses primarily associated with lithological changes:

- Gamma Ray log, which detects the natural radioactivity of the minerals,
- Spontaneous Potential log, which measures small electrical potentials at each depth between the formation and a grounded electrode at the surface,
- Bulk Density log, which uses gamma ray scattering using a radioactive source and a single detector. The measurement is a result of the grain density of the varying minerals and the pore space. The combination of bulk density and neutron (*i.e.,* measures the hydrogen count in the formation) or sonic logs (*i.e*., measures the compressional velocity, impacted by mineralogy) enables the differentiation of the lithology.

Shale volume estimates (which generates sand volume estimates) for the Injection Zones were used to identify the permeable strata by using the GR and SP logs. However, identification of shale volume using the SP logs is limited to wells with conductive borehole fluid (*i.e.,* water-based muds and saline brines) and sparse insufficient GR log coverage. Permeable strata were also identified using the deep Resistivity curves from Laterolog or Induction tools (tools applied depending on the drilling mud type). These tools are used to measure the electrical conductivity in the formation and, through different petrophysical models, the formation saturation. An increase in resistivity values can be indicative of hydrocarbons, a lower total dissolved solids (TDS) content in the formation, and impermeable layers. The range of clay electrical conductivity is relatively constant (depending on clay type) and associated to the intrinsic clay bound water and salinity. In brine saturated formations there is lower uncertainty associated with the fluids in the pore system, therefore variations in conductivity can be associated with textural characteristics such as grain size, pore volume, and pore throat size.

Two rock types were modeled for the Vernon One CCS Site, which are sands and shales.

The first method employed using the Vsh cutoff method. Logs were uploaded into Techlog©, which is an integrative software program available from Schlumberger. This software program was developed to allow the user to evaluate and interpret well log data and integrate core data. Techlog©, was used to evaluate the petrophysical parameters that were then used to populate the static model.

Different shale volume cutoffs were investigated to determine presence of permeable layers in the injection zone. Without site specific calibration and seismic tie ins, the Vsh is used only as a qualitative indicator of permeable zones, therefore no corrections were applied. After establishing the permeable layers, total porosity was then calculated from density and sonic logs. (see **Section 3.2**).

The second method used to calculate a net sand utilized the Spontaneous Potential or Gamma Ray (depending upon availability), and Resistivity Logs. **Figure 8** details the manner in which sand was counted over a portion of the Bentley A-1 well (as an example). The resistivity was shaded at or below a cutoff of 1.1 ohm-m. This was then overlain with the SP (and GR where available). To be counted as sand the interval needed to satisfy two conditions: first the resistivity needed to be at or below the 1.1 ohm-m cutoff (now shaded yellow in **Figure 8**); second, the SP needed to be above the shale baseline. Additional considerations included the GR log (if available) and its position relative to the SP curve. The results from the SP baseline determination were then upscaled in the static model for the two rock types (sand and shale).

2.3 POROSITY

Porosity is defined as the ratio of void space to the total bulk volume of rock. It is expressed as a percentage (Amyx et al., 1960). There are different porosity types, traditionally siliciclastic systems deal with primary intergranular porosity (i.e., the void space that is preserved between the grains because of the fluid content), but complex porosity types (i.e., secondary porosity) exist as a result from dissolution and other mineral altering processes in carbonate systems, among others. Intergranular porosity is subdivided into the macro porosity space as well as a micro porosity space. Total porosity is the ratio of pore volume to the total volume of the rock. Effective porosity is the ratio of interconnected pore volume to the total volume of rock.

The porosity type is highly dependent on the mineral composition of the rock and defines how much pore volume is accessible to reservoir fluids, *i.e.* ratio of total and effective porosities. Primary intergranular porosity results from preservation of pore space after deposition and lithification of sediments. Microporosity, which is associated with clays, is present in the matrix and greatly affects the volume of effective porosity accessible to reservoir fluids.

Ideally, the static model should contain effective porosities to estimate a representative volume accessible to fluids. However, effective porosity quantification requires calibration obtained from Nuclear Magnetic Resonance (NMR) measurements. In the absence of NMR data, effective porosities can be estimated from shale volume content with a large degree of uncertainty given that the clay type influences the degree of clay-bound and capillary-bound volumes. Due to limited sample measurements and advanced log availability, total porosity values are used in the model and discounted by using a saturation height function, derived from capillary pressure measurements.

Three bulk density logs were available for analysis near the Vernon One CCUS Site (see **Table 4** and **Figure 1**). Porosity from density is considered the most representative porosity estimate in the formation, followed by the sonic porosity estimate. Sonic porosity estimates require additional calibration introduced by fluid content as the measurements are affected by the grain framework as well as the saturating fluids to a larger extent. Porosity estimate from neutron logs are not considered individually representative as clay bound water (CBW) introduces excess porosity due to its hydrogen response. Clay bound water is part of the clay matrix structure and although it appears as part of the total porosity, it is pore space that is inaccessible to fluids therefore not part of the effective pore volume.

The density porosity equation was used to estimate the most representative porosity values. It uses the bulk density log (r_{bulk}), which varies by depth. The matrix density (r_{ma}) is normally obtained from core measurements; however, these were not available within the regional core. Instead, lithological core sample descriptions showed a range of clean sands to shales in the injection to containment zones (*i.e.* simple lithology). Assumption of a single lithology for total porosity estimate was suitable for all targeted zones. Fluid density (r_{fluid}) is based upon the salinity of the fluid present in the invaded zone, which is composed of a mixture of reservoir fluids and mud filtrate to the extent that it invades the reservoir while drilling.

$$\emptyset_{density} = \frac{\rho_{matrix} - \rho_{bulk}}{\rho_{matrix} - \rho_{fluid}}$$

Where:

$\emptyset_{density}$ total porosity

ρ_{matrix} mean density of the matrix minerals

ρ_{bulk} bulk density

ρ_{fluid} density of the fluid

A fluid density of 1.0 g/cm^3 was assumed for the invaded zone. This density value for the fluid was selected to represent the mud filtrate and formation fluid mixture within the invaded zone. Matrix density is assumed to be 2.65 g/cm^3 for sandstones using standard industry measurements.

Core porosity measurements from the Hanna well were used to calibrate the core grain density and fluid density assumptions. The comparison indicates that the selected parameters are representative of the porosities in the reservoir within an acceptable uncertainty (**Figure 9)**

Porosity measurements were also estimated using the Raymer Hunt equation for five sonic logs. This method employs using reference matrix compressional slowness values for sand and a representative regional shale combination.

$$\emptyset_{sonic} = C\frac{\Delta t_{log} - \Delta t_{matrix}}{\Delta t_{log}}$$

Where:

$\emptyset_{sonic}$ total porosity

C 0.625 (also represented as 5/8) constant factor

Δt_{log} sonic response at depth of interest

Δt_{matrix} response associated with matrix

Sonic logs analysis is dependent on estimating the formation pressures and the compressibility of the material. As these site-specific parameters are estimated, the total porosity values from the sonic logs are considered conservative.

Additionally, core derived measurements were used for the calibration of the porosity in the log estimates. Core measurements used in the log estimate calibration described above showed a porosity range as follows:

Table 9 - Total Porosity Measurements from Available Core

Formation	Minimum Porosity*	Maximum Porosity*
[redacted]	14 %	40 %
[redacted]	17 %	39 %

Core data was not available from the [redacted], therefore log porosity estimates have slightly larger uncertainty than the [redacted] core calibrated porosity model. Assumptions were made on porosity preservation/compaction mechanisms based on regional geology as well as log response. Because core measurements are used as calibration, it is implicit that the estimation parameters are adjusted in the future using additional data acquired during the drilling and testing on the injection wells, to close the gap in the iterations.

Additionally, shale porosities were reviewed as part of the seal efficiency assessment with the end goal in mind to estimate permeabilities and entry pressures (via understanding textural components such as pore throat size). Although log evaluation in the shales can indicate high total porosity, a review of published literature was used to determine shale effective porosities as an indicator of the clay bound volume. No core data is available to calibrate shale porosity in this region at this stage but will be addressed as part of the future data collection.

Effective shale porosities developed for Gulf Coast shales are presented in Porter and Newsom (1987) (**Table 10**). These minimum effective shale porosities decrease as a function of depth due to lithification and no local overpressures are assumed.

Table 10 – Minimum Effective Shale Porosity in Gulf Coast Environments

Depth (feet)	Porosity (%)
1,000	18.0
1,500	15.5
2,000	13.5
2,500	12.5
3,000	12.0
3,500	11.5
4,000	11.0
5,000	10.5
6,000	9.5
7,000	9.0

(Table 2, in Porter and Newsom, 1987)

The "effective" shale porosity, which discounts the bound water within the clay structure as well as water contained in dead-end pores, represents an appropriate choice of a porosity value for such a calculation. Using the (Porter and Newsom, 1987) relationship for the minimum effective porosity in a shale versus depth, the maximum porosity in the shales is expected to range between 11 percent for shales above the uppermost injection zone ([redacted]) and 9 percent for shales within the lowermost injection zone ([redacted]). Effective porosities are expected to be less than 9 percent below the [redacted]. These values were used along with the published permeability values to characterize the containment units in the static model.

To model the porosity, the well log data was first upscaled at the well to the model layering. A detailed workflow for the how the porosity was assigned in the model and distribution is detailed in **Appendix 3.1** of this report. The process of upscaling was done using a simple arithmetic mean. The data from the

upscaled well logs was then distributed within the model utilizing a simple sequential gaussian simulation.

Section 3.3.1 within the Appendix 3.1 presents the histograms of the Total Porosity data in three states: 1) that of the raw well log data; 2) the range in the upscaled cells; and 3) the range in the model populated property. Over the [redacted] interval the histogram shows that the Total Porosity well log data spans a range of 0.233 to 0.347 porosity units, with an average of 0.3. For the [redacted] interval, the Total Porosity well log data spans a range of 0.142 up to a maximum of 0.3 porosity units and an average of 0.239 porosity units. Finally for the [redacted] interval the Total Porosity well log data spans a range of 0.068 up to a maximum of 0.267 porosity units and an average of 0.191. All the data for these three injection intervals can be found in the Tables accompanying the Porosity Data Histograms (**See Appendix 3.1**).

This wide data range is the result of log porosity being the total porosity, as there is not sufficient data to calculate an effective porosity at this time. However, a future test well will be designed with this in mind, and the appropriate data will be collected so that an effective porosity can be calculated.

The porosity logs for each of the Injection Intervals ([redacted]) were upscaled using a simple *arithmetic average*, with the log data sampled by treating the log as lines and *neighbor cell* used for the manner in which the cells penetrated by wells were sampled for the upscaling process. Through this process of well log upscaling, the range of porosity values over the injection interval is tightened. The impermeable layers were set at a porosity of zero. The upscaled cells and resulting model populated total porosity values for the [redacted] injection interval was truncated at a minimum of 0.2338 and maximum of 0.3391 porosity units. The upscaled cells and resulting model populated total porosity values for the [redacted] were truncated at a minimum of 0.1427 and a maximum of 0.3005. The [redacted] upscaled cells and resulting model populated total porosity values range from a minimum of 0.0689 to a maximum of 0.2678 porosity units.

It should be noted that while the porosity distribution in the [redacted] yielded what appear to be relatively normal distributions, the [redacted] distribution clearly indicates the possibility of a bimodal porosity distribution. This will need to be investigated thoroughly in the collection of data for a site specific well to be drilled in the future.

Results of the porosity data distribution, the specific histograms can be found for the [redacted] contained in **Appendix 3.1**. For all layers, Total Porosity was modeled using "*Gaussian random function simulation*".

The model assumed a single upscaled porosity value for each layer at each well containing a porosity log (using the limited data set). The distribution of the porosity is geographically heterogenous as is indicated by the porosity distribution maps that represent each layer in the static model (**Appendix 3.1**). **Table 11** contains the porosity ranges, by layer based upon the conservative analysis.

Table 11: Porosity inputs into the Model by layer:

[redacted]			
Model Layer	**Min Porosity (%)**	**Max Porosity (%)**	**Average (%)**
2	27	30	29
3	26	30	29
4	25	29	27
[redacted]			
6	22	28	25
7	15	22	17
8	16	25	22
9	20	26	23
10	14	16	15
[redacted]			
12	11	22	19
13	7	16	12
14	9	21	17
15	11	21	15
16	7	16	12

**Note – impermeable layers were assigned a 0% porosity*

Initial data indicates that Injection Zone 1 – [redacted] contains the highest porosity with the porosity decreasing with depth into Injection Zone 3 – [redacted].

The three impermeable boundaries modeled are the [redacted]. The lower confining zone is the [redacted], which does not have impact on the flow of the CO_2 (which is mobile vertically in the reservoir formation and updip geologically). Each of these layers were assigned a value of zero porosity, zero permeability and zero feet of net sand within the model. Upon the drilling of stratigraphic test well for the project, data for these intervals will be collected to verify the impermeability of these layers.

CapturePoint, LLC is currently drilling a stratigraphic test well. Data to be collected from this well include core, fluid samples and logging suites. Data collected from this well will be used to calibrate and update the porosity determinations for the Vernon One CCS Site. Site specific data regarding the porosity of the injection intervals and confining zones will be collected during the drilling of stratigraphic test well and injection wells.

Details on the data acquisition plan for the site are contained in "*D. Pre-Operational Testing Plan*" submitted in **Module D**. The additional core data and logs will reduce the uncertainties in the current model and refine the final pressure and plume front movement.

2.4 PERMEABILITY

Permeability is defined as the capacity of a porous media to transmit fluids (Amyx et al., 1960). High connectivity of the pore spaces provides the pathway for fluids or gasses to move through a formation, in either direction (vertical or horizontal). However, permeability is not an intrinsic rock property and varies depending on multiple factors such as the fluid content and textural components such as grain size, orientation, arrangement, cementation, clay content, grain size distribution and sorting. When two or more fluids are present within the pore space, immiscible displacement of one fluid by another affects the speed at which each fluid flows within the porous space (*i.e.* relative permeability). Immiscible displacement of brine takes place when CO_2 is injected into an aquifer in addition to the interaction of the brine and CO_2 (dissolution of one phase into another depending on the pressure and temperature conditions).

To model the CO_2-brine displacement, absolute permeability is first measured under representative in-situ conditions on core samples. Absolute permeability is a function of effective porosity, irreducible wetting phase saturation, displacement or threshold pressure corresponding to a pore throat radius, and basic pore size characteristics. Since porosity dominates the pore size characteristics more than any other textural component a porosity-permeability correlation can be used to estimate permeability from total log porosity. A correlation with log derived porosity is then established and applied to characterize all the target zones.

Absolute permeability is described by Darcy's Law. Calibration can be obtained from a range of sources: core measurements (plug scale), NMR (log resolution), Formation Pressure mobilities (connected flow units), Drill Stem and Fall Off pressure Tests (zones open to testing for flow):

$$q = -\frac{kA}{\mu}\frac{dp}{dL}$$

Where:

q = volumetric flow in cm^3/s

k = permeability in Darcy's

A = cross-sectional area in cm^2

m = viscosity in cp

Dp/dL = Pressure drop per unit length in atm/cm

Often core permeability measurements result in a wide range of absolute permeability values measured per porosity class. The range of permeability variations observed in each porosity class can be explained by variations in mineralogy, as effective porosity is greatly affected by clay type. This can be addressed by rock typing where sufficient calibration data is available. Regional core (total) porosity and permeability data was used to establish a correlation to estimate a continuous permeability log from the log porosities estimated where bulk density and sonic logs were available.

The interpretation was integrated as best possible with the local geological model to define mathematical functions representative of average permeability values (**Appendix 3.2**). Future data collection will address individual high permeability unit calibration through a range of measurements (e.g. core

measurements, NMR, MDT mobilities, well test). Each of these correlations were applied to the estimated porosity logs in Petrel and distributed per geological unit accordingly. Absolute permeabilities are distributed in the static model and are later supplemented with relative permeability functions in the dynamic model to simulate the CO_2-Brine flow.

For the injection reservoirs, a porosity-permeability transform was developed and added to the model in Reveal (**Table 12**).

Table 12: Porosity-Permeability Transforms used in the Reveal Model.

Injection Zones (Reservoirs)	Porosity-Permeability Transform
Injection Zone 1 – [redacted]	$K_{abs} = 10^{(9.58 \cdot \varphi - 0.3)}$
Injection Zone 2 – [redacted]	$K_{abs} = 10^{(9.58 \cdot \varphi - 0.3)}$
Injection Zone 3 – [redacted]	$K_{abs} = 10^{(11 \cdot \varphi - 1.15)}$

The five intervals modelled as confining zones and impermeable boundaries ([redacted]) were all treated as having a permeability of zero. These rocks will be tested in the drilling of a stratigraphic test well, and the model will be updated with that information. The justification assigning a value of 0 for permeability is based upon detailed reviews of regional literature, for ductile shales at similar depths, that illustrates their behavior as regional seals.

2.5 ROCK COMPRESSIBILITY

If the pressure in a formation increases, such as due to injection, or drops, such as due to fluid withdrawal, the skeletal matrix will expand or contract, respectively (Fetter, 1988). This elasticity in the skeletal matrix is known as compressibility (Fetter, 1988). Compressibility is a material property that describes the change in volume induced in the material by an applied stress. The native formation fluid volume will also expand or contract because of pressure changes in a formation.

Petroleum engineering generally handles three-phases being present within a formation. Therefore, total compressibility when there are three fluid phases is defined as:

$$c_t = c_f + S_o c_o + S_w c_w + S_g c_g$$

where:

c_t	=	total compressibility (psi^{-1})
c_f	=	formation compressibility(psi^{-1})
S_o	=	oil saturation (fraction)
c_o	=	oil compressibility (psi^{-1})
S_w	=	water saturation (fraction)
c_w	=	water compressibility (psi^{-1})
S_g	=	gas saturation (fraction)
c_g	=	gas compressibility (psi^{-1})

2.5.1 Formation Compressibility

For water-filled reservoirs, such as at the Vernon One CCS site, in which S_w equals 1, this simplifies to:

$$c_t = c_f + c_w$$

The change in porosity is a result of the elastic properties (or moduli) of the framework of the rock (i.e. the grain, cements and contacts). A large pore volume compressibility transfers pore pressure more effectively across the pore system, enabling fluids to percolate through. The rate of change in pore volume is influenced by textural components of different rock types. It is quantified by pore volume compressibility (cf). For unconsolidated formations, compressibility is defined as the change in pore volume, not just porosity (Wattenbarger, 1999):

$$c_f = \left({}^{1}/_{V_\emptyset}\right)\left({}^{\partial V_\emptyset}/_{\partial p}\right)$$

A large pore volume compressibility transfers pore pressure more effectively across the pore system, enabling fluids to percolate through. The rate of change in pore volume is influenced by textural components of different rock types. It is quantified by pore volume compressibility (c_f). Values for formation compressibility (c_f) in these unconsolidated sediments generally fall in a range between 20×10^{-6} psi^{-1} to more than 100×10^{-6} psi^{-1} (Wattenbarger, 1999; Newman, 1973). Newman (1973) found that in unconsolidated sands, pore-volume compressibility tends to increase with porosity, with measured values in excess of 90.0×10^{-6} psi^{-1} for unconsolidated sands with porosity greater than 30 percent (Wattenbarger, 1999; Yale et al., 1993). The values in unconsolidated sands have much greater compressibility than those measured in well-cemented, consolidated rocks. The injection zones at the Vernon One CCS site are expected to fall into the unconsolidated to slightly consolidated sands typical of the Gulf Coast region.

Compressibility inputs into the model for the injection zones used for the model are contained in **Table 13:**

Table 13: Compressibility for the Injection Zones

Injection Zones (Reservoirs)	Formation Compressibility
Injection Zone 1 – [redacted]	3.1×10^{-6} psi^{-1}
Injection Zone 2 – [redacted]	2.9×10^{-6} psi^{-1}
Injection Zone 3 – [redacted]	2.4×10^{-6} psi^{-1}

Future data and calibration for compressibility will be obtained from testing of the core material. Calibration is obtained as part triaxial tests on vertical samples, which are designed to estimate the Biot coefficient (*i.e.* the fluid volume change induced by bulk volume changes in the system). To measure bulk compressibility, the vertical sample is loaded isostatically and a constant pore pressure is applied, changing the effective stress on the sample. Strains are monitored and used to estimate volumetric strain. These measurements for total bulk compressibility will be used to reduce uncertainties for the overall compressibility of the material. It will also provide refinement into the model.

In the Gulf Coast, clay layers are more compressible than sand layers (Kasmerek et al., 2010; Kasmerek and Ramage, 2017). Confining shale compressibility (a) is conservatively assigned to be an order of magnitude higher than the sand layers. These higher compressibilities for the clay layers are consistent with observations from depressuring and dewatering of clay layers because of groundwater withdrawal. Under withdrawal, not only is a load placed on the clay layer skeleton framework, but this load also produces a reorientation of the plate-like clay grains perpendicular to the load (Kasmarek, 2012).

Note, that since the shale confining layers are made to be impermeable in the model, the exact choice of compressibility value in the confining layer is not pertinent to the prediction of the pressure buildup with time.

2.5.2 Formation Fluid Density, Compressibility and Viscosity

Density

Brine compressibility (c_b) represents the change in volume (∂V_b) of the brine, relative to initial volume (V_b), for a given pressure change (∂p) at constant temperature.

$$c_b = \left({}^{1}/_{V_b}\right)\left({}^{\partial V_b}/_{\partial p}\right)$$

Compressibility can also be defined based on the change in density (∂V_b) of the brine, relative to initial density (ρ_i), for a given pressure change (∂p) at constant temperature, assuming mass is conserved.

$$c_b = \left({}^{1}/_{\rho_i}\right)\left({}^{\partial \rho}/_{\partial p}\right)$$

The highest possible brine density is used in the model to create a conservative (largest) estimate of plume size and movement. In general, a larger density difference between the in-situ fluid and injected CO_2 increases the predict plume size, and buoyancy velocity. Velocity of the CO_2 phase can be estimated analytically using the equation as noted in reference [i] .

$$U = \Delta\rho g k \,/\, \phi\mu l$$

In the equation, U = Darcy velocity due to buoyant force, $\Delta\rho = \rho h - \rho l$, is the density difference between the heavy (brine) and light (CO_2) phase, g is the gravitational constant, $k/\mu l$ is the mobility of the light phase and is ϕ porosity.

With respect to the fluid density used in the model, each of the proposed injection zones are assumed to be initially saturated with native formation water having specific gravity of 1.1 and density of approximately 68 lb/gal at standard conditions. The in-situ brine is assumed to be comprised of primarily of NaCL. This density yields a pressure gradient in line with the highest gradient values observed in the regional pressure data trends.

For comparison, using nominal [redacted] conditions, the density of water at 2,000 psi and 131˚F is approximately 64.2 lb-m/ft3 using NaCL of 50,000 ppm, compared to 68 lb-m/ft^3 (SG = 1,1). With nominal CO_2 density of 40 lb-m/ft^3 the buoyancy velocity is 18.5 percent (68.7 /64.2) greater in the presence of the heavier brine.

The higher density also produces higher initial pressure in the grid. This yields a more conservative estimate of maximum rate that can be achieved without violating fracture initiation pressure. In addition,

the higher density creates a more conservative (bigger) estimate of the Cone of Influence and Area of Review

The estimated in-situ brine density used in the model is estimated at specific temperature and pressure using an internal correlation provided by Petroleum Experts (PETEX). The graph in **Figure 10** shows the initial density estimated at nominal formation temperature, over a range of pressure, for each of the injection intervals using the internal PETEX correlation.

Viscosity

The Revel model uses an internal correlation to estimate water viscosity as described in the User's Manual. The viscosity calculation is also dependent upon pressure, temperature and density. As mentioned previously, the in-situ water density is assumed to be greater than that estimated from formation resistivity. This higher density increases viscosity by approximately 18 percent (0.724 cp /0.614 cp) which in turn yields a lower effective mobility to water. More force is required to displace the higher viscosity brine thus creating a larger pressure build-up during the injection process.

The table and graph below show water viscosity calculated using specific gravity of 1.1, at nominal pressure and temperature conditions for each of the three injection layers.

Table 14: Initial Viscosity at Nominal Conditions

Zone	Pressure (psia)	Temperature (˚F)	Viscosity (cp)
[redacted]	1,809	126	0.759
[redacted]	2,187	138	0.679
[redacted]	2,920	162	0.555

Density (compressibility) and viscosity are a function of pressure and temperature (See graph in **Figure 11**). Therefore, a range of density values are encountered throughout the modeled grid space. **Figures 12, 13, and 14** illustrate the expected pressure and temperature distribution in the grid at the top and bottom layers for each Injection Zone for the formation fluid.

2.6 CONSTITUTIVE RELATIONSHIPS

Relative permeability behavior and capillary trapping characteristics of both the confining zone and impermeable boundary are recognized as highly impactful to the ability to inject and immobilize supercritical CO2 within the storage complex. The forces that govern fluid flow in porous media are viscous forces, effects of gravity and capillary imbibition. Fluid flow models are based on the law of conservation of mass, described by Darcy's law.

The rate of displacement of the brine by the CO2 as well as the extent of the plume require dynamic reservoir modelling based on the initial static model. Hydraulic and structural trapping mechanisms of CO2 sequestration apply under two phase flow displacement. In porous media containing two phases, one of the two phases will have a tendency to contact a wider surface area of the grain compared to the other phase. The parameter that measures this tendency is defined as wettability; the phases are classified as wetting or non-wetting. The brine is the wetting phase in a CO2 – brine system. The wetting phase is able

to access the smallest pores, while the non-wetting phase is limited to the largest connected pore space. Continuous fluid percolation through pores results in flow of the individual phase. The non-wetting phase in this model, the CO2, may become disaggregated into separate isolated volumes. The relative permeability of each phase is the ratio of the phase's effective permeability to the absolute permeability and depends on the complexity of the pore system, absolute permeability, wettability, and interfacial tension between the two fluids. Darcy's law incorporating multiphase flow is used to forward model individual phase flow, with capillary pressures and relative permeability being the key parameters to introduce the two fluids in the system:

$$q_i = -\frac{k * k_{ri}(S_i) * A}{\mu_i} \frac{dP}{dx}; i = (w, nw)$$

Where:

k	absolute permeability
k_i	relative permeability to phase
S_i	volume fraction of fluid in pore (saturation)
q	flux of the phase (m^3/s)
μ	viscosity of the phase
A	area cross section
dP/dx	pressure gradient over the interval

Indices *w* and *nw* refer to wetting and non-wetting phases.

The model includes a drainage process (CO_2 displacement of reservoir brine), assuming that imbibition is not present (no evidence of local hydrologic recharge). A Brooks-Corey relationship, for the relative permeabilities, was based on literature analogues. The following exponents (**Table 15**) were used as inputs for the dynamic reservoir model

Table 15: Relative Permeabilities and Saturation Factor inputs into Reveal

Phase	Critical Fluid Saturation	Brooks Corey Endpoint	Brooks Corey Exponent
Brine	S_{wc}= 0.25	0.8	2
Gas	G_{cs}=0.05	0.8	2

2.7 BOUNDARY CONDITIONS

No major geologic boundaries, such as faults, have been identified within any of the confining or injection zones in the study area. However, pore volume multipliers have been added to the perimeter of the entire Reveal grid system. This methodology mimics a constant pressure boundary at the grid edges. The pore volume multiplier has been applied to the outer two cell blocks across all the layers.

The pore volume multipliers effectively create a constant pressure boundary as evidenced by the spatial distribution of injection pressure within the grid system. There is minimal pressure build-up at the edges of the grid.

2.8 INITIAL/STATIC CONDITIONS

Initial conditions for the model and each injection interval are given in **Table 16 through 18**. Initial conditions are based upon offset well data, regional data, and literature sources relevant to the injection formations.

The temperature gradient, and its uncertainty range, used in the Reveal model was taken from published data as there is no measured data for the Vernon site. A gradient (1.49° F/100 ft), and a mean annual surface temperature in Vernon Parish of 67 °F, the estimated subsurface temperature for each interval.

Salinity was calculated by using the general theory in determining water quality in clean water-bearing zones flows from the formation water resistivity (R_w), which can be calculated by using the Archie equation (Schlumberger, 1988). Resistivities of saline solutions vary as a function of NaCl concentration and temperature. The relationship between temperature, NaCl concentration, and resistivity are typically determined by using the Schlumberger Gen 9 Nomograph.

Formation pressures were determined by evaluating field pressures available for 40 reservoirs ranging in depths from 3,759 feet to 7,648 feet in the near region. A best-fit linear trendline indicates pore pressures of 0.455 psi/foot of depth. The gradient for the Vernon Parish is set at 0.455369 psi/ft tvd-ss and the formation pressures are calculated at top of the injection zone formation.

Table 16: Initial conditions for the [redacted]

Parameter	Value or Range	Units	Center Grid of Dynamic Model Layer 1 Elevation (ft MSL)	Data Source
Temperature	126	F	3,975	Burke et al. 2020
Formation pressure	1,809	psia	3,975	0.455 psi/ft per regional pressure
Fluid density	1.1	SG	--	Conservative Value to match Pressure gradient

Table 17: Initial conditions for the [redacted]

Parameter	Value or Range	Units	Center Grid of Dynamic Model Layer 1 Elevation (ft MSL)	Data Source
Temperature	138	F	4,807	Burke et al. 2020

Parameter	Value or Range	Units	Center Grid of Dynamic Model Layer 1 Elevation (ft MSL)	Data Source
Formation pressure	2,187	psia	4,807	0.455 psi/ft per regional pressure
Fluid density	1.1	SG	--	Conservative Value to match Pressure gradient

Table 18: Initial conditions for the [redacted]

Parameter	Value or Range	Units	Center Grid of Dynamic Model Layer 1 Elevation (ft MSL)	Data Source
Temperature	162	F	6,417	Burke et al. 2020
Formation pressure	2,920	psia	6,417	0.455 psi/ft per regional pressure
Fluid density	1.1	SG	--	Conservative Value to match Pressure gradient

Formation temperature and pressures are expected to increase with depth. No lateral spatial disparity is expected in the salinity or density of the formation fluids. Salinity of the formation fluids is expected to increase with depth. No lateral spatial disparity is expected in the initial static conditions. Initial conditions will be updated with data acquired during the drilling of the stratigraphic test well and injection wells (See "*D. Pre-Operational Testing Plan*" in Module D). The additional core data and logs will provide baseline measurement and be used to update the model.

2.9 OPERATIONAL INFORMATION

Details on the injection operation are presented in **Tables 19 thru 21**. These are the values used in the model based upon the initial designed program and expectations. Note: as this project evolves, the operational input information will be refined based upon actual site-specific data, the as-built well construction, and permitted injection operations.

Table 19: Operating details for Injection Zone 1 - [redacted]

[redacted]

[redacted]

Table 20: Operating details for Injection Zone 2 – [redacted]

[redacted]

Table 21: Operating details for Injection Zone 3 – [redacted]

[redacted]

[redacted]

2.10 FRACTURE PRESSURE AND GRADIENT

No site-specific data is currently available for the fracture gradient. However, the fracture gradient for the Vernon Parish site was estimated using Eaton's Method (Eaton, 1969) and the methodology presented in Moore (1974).

$$FG = \frac{(P_{ob} - P_r)e}{(1 - e)} + P_r$$

Where:

FG	=	Fracture Gradient
P_{ob}	=	Overburden Gradient (Figure 11-11 in Moore, 1974) - depth dependent
P_r	=	Reservoir Pressure Gradient (original)
e	=	Poisson's Ratio (Figure 11-12 in Moore, 1974) – depth dependent

The nomographs presented in Moore (1974) are solved for all injection intervals at the Vernon Parish site using the top of the formations in the offset well [redacted]. An example calculation is included for the shallowest Injection Zone 1 – [redacted]:

$$FG = \frac{(0.9042 - 0.455) * 0.3983}{(1 - 0.3983)} + 0.455$$

$$= \quad 0.75 \text{ psi/ft}$$

A fracture gradient was then obtained for each of the remaining injection zones using the estimated top of formation as presented in **Table 22**.

Table 22: Calculated Fracture Pressure

Injection Pressure Details	[redacted]	[redacted]	[redacted]
Estimated Fracture gradient (*psi/ft*)	0.75	0.77	0.81
Depth to top of formation (*ft tvd-ss*)	3,975	4,807	6,417
Calculated Fracture Pressure (*psi*)	2,981	3,701	5,198

These initial estimates are very conservative in nature are based upon available and using literature sources.

Figures 41 thru 43 show the calculated fracture gradient (blue line), the safety factor of 90% of the gradient line (green line), and the pressures based upon the injection rates for the Vernon One CCS Site (red line) for each of the injection formations at a decreasing depth. *Note:* each modeled injection zone remains less that the 90% safety factor for the modeled timeframe.

CapturePoint will operate with injection pressures set at 90 percent of the fracture gradient identified for each formation. This provides an additional level of safety. Using this gradient, the following values for each layer in the model **(Tables 23 thru 25).**

Table 23: Injection pressure details – [redacted]*

Well No.	**Injection Rate (mmscfd)**	**Top layer/Center Grid Depth (ft tvd-ss)**	**RED LINE Modeled Injection Pressure (psia)**	**GREEN LINE Fracture Pressure with 90% Safety (psia)**	**BLUE LINE Fracture Pressure (psia)**
MT_S_1	[redacted]	375	2,042	2,683	2,981
MT_S_2	[redacted]	3992	2,039	2,695	2,994

Please see **Figure 15 – graph plot of fracture and injection pressures for each well with depth*

Table 24: Injection pressure details – [redacted]*

Well No.	**Injection Rate (mmscfd)**	**Top layer/Center Grid Depth (ft tvd-ss)**	**RED LINE Modeled Injection Pressure (psia)**	**GREEN LINE Fracture Pressure with 90% Safety (psia)**	**BLUE LINE Fracture Pressure (psia)**
MT_UW_1	[redacted]	4,807	2,919	3,331	3,701
MT_UW_2	[redacted]	4,857	2,943	3,366	3,740

Please see **Figure 16 – graph plot of fracture and injection pressures for each well with depth*

Table 25: Injection pressure details – [redacted] *

Well No.	Injection Rate (mmscfd)	Top layer/Center Grid Depth (ft tvd-ss)	RED LINE Modeled Injection Pressure (psia)	GREEN LINE Fracture Pressure with 90% Safety (psia)	BLUE LINE Fracture Pressure (psia)
MT_LW_1	[redacted]	6,417	4,262	4,678	5,198
MT_LW_2	[redacted]	6,490	4,333	4,731	5,257

Please see **Figure 17 – graph plot of fracture and injection pressures for each well with depth*

The model was run to confirm that the pressures predicted to occur within the geologic system will not exceed 90 percent of the fracture pressure of any of the injection zones. Currently, the estimated top of the expected perforations is unknown and variable, especially in the [redacted] intervals. The depths of the perforations will be dependent on the open hole logging analysis after the injection wells are drilled. The perforation tops will be injection well specific.

Additionally, the fracture gradient will be obtained for each injection zone during the drilling and testing of the injection wells. Tools such as the MDT (modular formation testing tool) can be acquired during *in-situ* open hole testing. The test slowing increases the pressure in the target formation until it breaks and provides a direct measure of fracture pressure. The rate of pressure bleed off is then analyzed to indicate the closure pressure. This data is then used to determine the site-specific maximum injection pressure (still within the 90% safety margin) for each well.

Details on the data acquisition plans are contained in "*D.1 – Pre-Operational Testing Plan*" submitted in Module D and includes the fracture gradient determination. The results in this initial model report are conservative is estimation and will updated data is available. Site specific results are expected to yield a slightly higher fracture gradient and allow for higher injection pressures.

2.11 CHARACTERISTICS OF THE CO_2 STREAM

2.11.1 CO_2 Density and Compressibility

All modeling presented in this submittal assumes 100% CO_2. The CO_2 density and phase behavior are estimated using the Penguin Robinson Equation of State (EOS). The Peng-Robinson method is used throughout the petroleum and chemical industries to model the phase behavior, molar volume (density) of single and multi-component systems.

The CO_2 critical pressure, and critical temperature used in the Peng-Robinson EOS **(Table 26)** for this study are consistent with values provided by the National Institute of Standards and Technology (NIST) for CO_2.

Table 26: Property inputs for CO_2

Parameter	Input Unit
Critical temperature (Tc)	87.7608 ˚F
Critical pressure (Pc)	1,070.0 psia

The graphs contained in **Figures 18 through 20** show the CO_2 density (graphs) estimated for each of the injection intervals at the initialization temperature and range of pressures. The graphs compare estimated CO_2 density calculated using the Peng-Robinson EOS, implemented in the Reveal software, with the density estimated using the Span, Wagner EOS implemented in the NIST Webbook. There is good comparison between the two EOS methods.

CO_2 density increases as pressure increases and decreases as temperature increases. Because of this relationship, the density of the CO_2 in each of the injection zones is similar. For instance, the [redacted] pressure is higher than the [redacted] which would create a higher density plume, however, temperature is also higher which decreases CO_2 density. The density of the plume, especially at the leading edge of the plume, is of interest. The density contrast between the CO_2 and in-situ water, along with the formation dip influence potential plume migration. The plume density at the leading edge for each injection zone are shown in **Figures 21 through 23.**

The plume density at the leading edge is approximately 615 kg/m3 (38.3 lb-m/ft^3) for the [redacted] (**Figure 21**), 670 kg/m3 (42 lb-m/ft^3) for the [redacted] (**Figure 22**), and 700 kg//m3 (43.7 lb-m/ft^3) for the [redacted] (**Figure 23**).

2.11.2 Viscosity

CO_2 viscosity is estimated using an implementation of the Lohrenz, Bray Clark method within the Reveal Model. The graphs in **Figures 24 through 26** estimated super-critical CO_2 viscosity at nominal pressure and temperatures for each of the three injection zones. The values estimated within the Eclipse software are then compared to values estimated using the NIST webbook, which implements the method of (Laesecke and Muzny, 2017) to estimate viscosity.

2.11.3 CO_2 and Formation Interactions

It is known that CO_2 and water will form Carbonic Acid (H_2CO_3) which in turn has the capability to dissolve calcium species in the formation. This can alter formation permeability and porosity depending on the native mineralogy.

This study does not consider CO_2 reaction with the formation currently. Future modeling will consider these aspects given the results of core and petrophysical analysis obtained from the site study well. From the nature of expected CO_2 sources and the pipeline specs, the injected CO_2 will have 96 percent or higher purity. The remaining elements are expected to be mostly Nitrogen, some trace hydrocarbons and H_2S, less than 100 ppm. Of these non- CO_2 components, only H_2S is expected to be potentially reactive, but at this low concentration it is too dilute to be reactive. The other impurities are at levels insignificant to affect general behavior of CO_2. It has been CP-CPS collective experiences from three decades of operating more than 15 Gulf Coast tertiary CO_2 floods that the other elements present has not affected expected reservoir behavior.

2.11.4 Solubility

The injected CO_2 at the Vernon One CCS site is expected to be soluble in water, which can provide a significant CO_2 trapping mechanism. This feature affects the reservoir by causing the higher density brine to sink within the formation thereby trapping the CO_2-entrained brine. This dissolution allows for an increased storage capacity and decreased fluid migration.

This has not been considered in this initial model iteration but will be considered in future modeling.

3.0 COMPUTATIONAL MODELING RESULTS

3.1 PREDICTIONS OF MODEL BEHAVIOUR

The model primarily considers advective transport of injected CO_2 into each of the injection intervals: [redacted]. Each of the intervals have been modeled separately since injection wells are specific to each interval and the model confines flow within the specified interval.

The model investigates the potential impacts of the Vernon site, which is the focus of this application, and at a proposed site ~18 miles to the east. Model results such as plume extent and pressure build-up are dependent on the geologic conditions assigned to the model (structure, thickness, porosity, permeability), and fluid properties (viscosity, density). In addition, the injection rate (volume & mass) will impact the pressure build-up at the well and in the surrounding reservoir. The volume (rate and duration) impacts the ultimate plume extent.

This study assumes there are two wells injection simultaneously, into each injection interval, at the Vernon site and at a site ~18 miles to the east (Rapides Parish Site referenced as "RP"). The maximum injection rate into the well has either been limited by the plume extent, well design or maximum allowable fracture initiation pressure. In all cases, skin is assumed to be zero and the well fully penetrates the formation.

Injection into the [redacted] was limited to [redacted] per day to limit plume extent. [redacted] properties allow high injection rates without reaching fracture pressure with a 90% safety factor. However, injection was reduced to limit plume extent due to the smaller net zone height in the [redacted].

Injection into the [redacted] was limited to [redacted] per well design. The large injection net interval and relatively high kh create low resistance to injection in the well and reasonable plume size. The plume extent is approximately the same as the [redacted], yet injection is [redacted] in the [redacted] compared to [redacted] in the [redacted].

Injection into the [redacted] wells are constrained by maximum allowable injection pressure in Rapides and max rate of [redacted] at Vernon Parish. In the case of the [redacted], the maximum allowable downhole injection pressure at the Rapides site was specified and the model used the pressure constraint to determine the allowable injection rate. At the Vernon Parish site, the focus of this submission, combined constraints are imposed; max rate of [redacted] and max allowable injection pressure. Although the net zone height is significant, the anticipated lower permeability creates a greater pressure buildup for a given injection rate. The constrained rate results in lower injection volume in the [redacted] and hence smaller plume extent.

Tables 27 thru 29 below summarizes the injection rate, maximum pressure, volumes and mass in each well. Note the CO_2 mass is in metric tonnes (1 metric tonne = 1,000 kg. and therefore 1kg = 2.204622 lb-m)

Detailed rate and pressure time series plots are provided in **Appendix 4** for each Injection Zone. Note that the Rapides Parish site was included to show the potential interfering effects between the sites.

Table 27: Injection Data for Wells complete in Injection Zone 1 - [redacted] Formation*

[redacted]

Time Series Plots* ***in Appendix 4 -* [redacted]

Table 28: Injection Data for Wells complete in Injection Zone 2 - [redacted] ***

[redacted]

Time Series Plots* ***in Appendix 4 –* [redacted]

Table 29: Injection Data for Wells complete in Injection Zone 3 - [redacted] *

[redacted]

Time Series Plots **Appendix 4 – [redacted]

The model allows injection into the entire layer, at each well, and CO_2 injection is distributed throughout the entire wellbore during the 20-year injection process. Since the model has no vertical barriers or baffles to prevent upward migration of the CO_2 within the injection zone, CO_2 migrates upward until it encounters the zone's confining layer. The largest accumulation of CO_2 occurs in the upper layer of each interval due to the density contrast between the CO_2 and the in-situ water. In addition, there is a prevailing, average, structural dip of approximately 1.3 to 1.4 degrees trending North (shallower) and 0.2 degrees West (shallower). This dip causes a slow migration of CO_2 primarily to the North at the Vernon site not only during the injection process but also during the post injection period which is discussed in Section 5.0 of this technical report.

3.2 MODEL CALIBRATION AND VALIDATION

Currently, data is not available for model calibration or sensitivity analysis. The initial model will be updated with site specific data acquired during the drilling of the stratigraphic test well and injection wells. Initial conditions and input parameters will be adjusted to reflect the data from site specific core and logs. The model will then be calibrated against history matching once injection operations commence. A model calibration will be performed prior to all AoR reevaluations.

The parameters used in the initial model iteration are conservative in lieu of site-specific data and is projected to be a "worst-case" scenario. A Sensitivity Analysis will be performed in the next model iteration using data acquired from a stratigraphic test well to meet the requirements pursuant to 40 CFR 146.93(c)(2(iv). Changes in the in-situ water density, composition, distribution of flow units, net thickness, properties such as porosity, permeability, and rock compressibility may yield changes in final pressure and plume growth rate and lateral extent at the end of the modeled 20-year period.

4.0 MODEL RESULTS

4.1 PREDICTED POSITION OF THE CO_2 PLUME

The approximate plume radius (saturation) in the upper layer, for each injection zone, is presented in **Appendix 5** at 5-year intervals. The time-periods are for 20 years of injection, with shut-in (post-closure) period of 50-years; total time series is 70-years.

- Appendix 5.1 - Injection Zone 1 – [redacted]
- Appendix 5.2 - Injection Zone 2 – [redacted]
- Appendix 5.3 – Injection Zone 3 – [redacted]

Inspection of plume saturation and pressure fields shows there is interference between the two injection wells at the Vernon site. In addition, there is minor distortion of the saturation field due to modeled injection from wells located at the proposed Rapides Parish site approximately 18 miles to the east. Initially the saturation plume extends radially from each well until the pressure front at the leading edge of each well's plume meet to create resistance to flow between the wells. The pressure resistance created by simultaneous injection between wells is expected and is extensively noted in pressure transient analysis (PTA) literature.

As time progresses the overall plume radius is much larger than the distance between the wells so that the two wells act as a single point of injection at the Vernon site. Since geology does not indicate the presence of faults or stratigraphic barriers near the injection site, and the structural dip is only slight, the plume extends nearly radially from the injection site after approximately 10 years.

As noted, injection migrates from the lower layers to the top layer(s), so the plume radius is much smaller in the lower layers but follows the same radial behavior. Cross sections at 5-year time intervals are also presented in **Appendix 5** which illustrate the vertical migration of CO_2 within each injection layer at the 5-year increments for the 20-years or injection and the 50-years of shut-in.

A more detailed analysis of the pressure-saturation profile is provided in **Appendix 6** which present key parameters and model results for each grid block in the North/South and West/East directions running through a representative well in each injection zone. Cross plots are presented that show Depth, Pressure, Temperature, CO_2 Saturation, calculated fluid properties (CO_2 and water density, viscosity). Values are shown for the top and bottom model layers and at selected time intervals; initialization, end of 20-year injection, and at 10-year increments post closure.

- Appendix 6.1 - Injection Zone 1 – [redacted]
- Appendix 6.2 - Injection Zone 2 – [redacted]
- Appendix 6.3 – Injection Zone 3 – [redacted]

The detailed values are used to summarize the plume extent along the North/South and East/West axis after 20 years of injection. The table below provides detailed model coordinates of the leading edge of the plume relative to a selected well in each zone. The modeled, absolute, plume extents at 20 years in the top layer, below the confining zone, are:

[redacted]

The plume radius shown is the distance between grid cells that have zero CO_2 saturation. The saturation images provide an approximation of plume extent, but by their nature, they don't exactly resolve the small saturation values at the leading edge.

Table 30: Absolute Modeled Plume Extent at 70-years, 50 years post closure – Top Layer

Absolute Modeled Plume Extent at 70 Years (50 Years Post Closure)

[redacted]

As mentioned, plume extent in the bottom layer is much smaller. The modeled, absolute, plume extent at 20 years in the bottom layer, are:

- [redacted]: 0.95 miles (N/S) by 1.52 miles (E/W) (**Figure 30**)
- [redacted]: 2.37 miles (N/S) by 1.61 miles (E/W) (**Figure 31**)
- [redacted]: 0.57 miles (N/S) by 0.57 miles (E/W) (**Figure 32**)

Table 31: Absolute Modeled Plume Extent at 70-years – Bottom Layer

Absolute Modeled Plume Extent at 70 Years (50 Years Post Closure)

[redacted]

Note the plume extent at 20 years in the bottom layer is essentially the same as at 70 years, 50 years post injection.

4.1.1 Ultimate Plume Extent

Analytical models from Celia and Nordbotton (2009) and Yamamotoa and Doughty suggest that within a *vertically* contiguous injection layer the plume is smallest at the base and extends asymptotically outward with the maximum extent at the boundary of the confining layer. The analytical approach can mathematically extrapolate the saturation profile to the near molecular level. The analytical model, however, is limited to simplifying assumptions regarding spatial distribution of properties.

The numerical model determines pressure and saturation in each grid block, with each grid block having its own volume and potentially unique properties (permeability, porosity). Additional layers in the numerical model can show the absolute extent of the plume to be greater than presented with fewer layers, depending on properties assigned to the grid. This effect is documented in various literature.

As noted previously, the [redacted] model incorporates 3 layers while the Upper and [redacted] models have 5 layers. All layers incorporate spatial variability of porosity and permeability. Each layer has been assigned a net-to-gross ratio and vertical permeability is 10 percent of horizontal permeability in all layers. The predicted plume extent would have been larger if more layers had been used in this model because this model is relatively homogeneous and allows a significant portion the CO_2 to migrate up to the confining layer.

Until Site wells are cored, the approach taken for the initial model iteration was a conservative assignment of minimal stratigraphic baffles or enhanced vertical continuity within the three injection zones. The plume extents presented above, are deemed to be reasonable based on the reservoir's current modeled homogeneity. It is expected that the site study well(s) will indicate additional complex heterogeneity within the current modeled layers and therefore will require additional vertical segregation between layers within each injection interval on the models second iteration. This increased vertical segregation will help distribute and diffuse the vertical movement of CO_2 and thus will reduce plume size.

In addition, this model does not include other aspects that mitigate plume extent such as saturation trapping (imbibition) and solubility trapping of the CO_2 in the in-situ water. These effects will be implemented once actual site data is obtained.

4.1.2 Plume Migration Post Closure

Post shut-in plume migration is primarily to the North of the injection wells due to regional dip and density contrast. There is essentially no migration to the South, nor to the East and West of the injection wells. Due to the dip, and the exclusion of physical behavior that mitigate plume migration in the model, the plume continues to drift at the rate of less than 100 feet per year. The rate of migration is estimated from the detail data referenced above.

Tables 32 thru 34 shows the northern plume extent at 10-year intervals, after injection stops, for each injection interval.

Table 32: Plume Migration Post Closure for Injection Zone 1 – [redacted] Formation

Year	dt Post Injection (years)	dx (feet)	dx/dt rate (ft/year)
20	--	--	--
30	10	1,500	150
40	10	2,000	200
70	30	7,000	233

Table 33: Plume Migration Post Closure for Injection Zone 2 – [redacted] Formation

Year	dt Post Injection (years)	dx (feet)	dx/dt rate (ft/year)
20	--	--	--
30	10	1,000	100
40	10	500	50
70	30	1,500	50

Table 34: Plume Migration Post Closure for Injection Zone 3 – [redacted] Formation

Year	dt Post Injection (years)	dx (feet)	dx/dt rate (ft/year)
20	--	--	--
30	10	500	50
40	10	500	50
70	30	500	17

It is expected that the inclusion of saturation trapping and imbibition in the model in future model iterations and using site specific data will show the plume stabilization. These features will be included using information provided by the site study well.

4.2 PREDICTED POSITION OF THE PRESURE FRONT

Appendix 7 shows the estimated pressure contours in the top layer of each injection zone starting with the initial pressure, and at 5-year increments. These pressure fields are the result of injection into two wells completed in the injection interval at the Vernon site. At the same time, 2 wells, with the approximately the same rate as the Vernon wells, are injecting at the proposed site 18 miles to the east.

- Appendix 7.1 - Injection Zone 1 – [redacted]
- Appendix 7.2 - Injection Zone 2 – [redacted]
- Appendix 7.3 – Injection Zone 3 – [redacted]

Because the formation is dipping the initial pressure is lowest in the Northeast corner of the grid and greatest in the Southeast corner of the grid. As injection is initiated the absolute pressure contours extend toward the shallowest part of the reservoir. This of course assumes kh (permeability-thickness) is approximately laterally the same near the well, which is the case for each of the injection intervals.

4.2.1 Net Pressure Build-up

Appendix 7 also shows the "net" pressure build-up contours at 5-year intervals for each injection layer. The "net" pressure is the difference in pressure created as a result of injection minus the initial pressure, at each grid cell. These contours indicate nearly radial pressure distribution around the well in early time. As injection increases, the influence of injection from the proposed site 18 miles east of the Vernon site is observed. The net pressure contour plots have been scaled to show the area near the Vernon wells.

4.2.2 Pressure Stabilization Post Shut-in

At the end of injection operations, pressure within the formation dissipates, but never completely returns to the initial pressure at the Vernon injection wells. This behavior is not the result of a pressure increase due to the increased mass injected into the grid, nor a grid effect. The net pressure at the edge of the grid would be elevated, or reduced, relative to the initial pressure if material balance influenced the behavior which is not the case. The contour shows the net pressure at the grid edge is zero in all cases.

Instead, the pressure increase observed in the vicinity of the well is a result of the CO_2 occupying the pore space in the region near the well instead of water. Pressure equilibrium is maintained within the overall grid as evidenced by the same initial and final pressure at the shallowest (**Figures 33, 34 and 35**) and

deepest part (**Figures 36, 37, and 38**) of the grid (North/South Pressure Cross Section portion of the figures). However, the redistribution of the heavier brine within the pore structure, replaced by less dense CO_2, results in a different pressure distribution near the well to accommodate the same hydrostatic potential between the shallowest and deepest parts of the grid. The pressure distribution is also a function of structure near the well.

5.0 AREA OF REVIEW

Under Environmental Protection Agency (EPA) 40 CFR 146.84 regulations, the Area of Review (AoR) is the area within which the owner or operator of a Class VI injection well must identify all artificial penetrations that penetrate the confining zone and/or injection zone and determine whether they have been completed or plugged so that they do not provide conduits for fluid movement. Artificial penetrations constitute a possible threat to human health or the environment because of their potential for conveying material out of the injection zone (no migration standard) and/or into an underground source of drinking water (USDW) (non-endangerment standard).

AoR delineation has been determined for the Vernon One CCS site using site characterization data, computational modeling data showing the projected lateral and vertical migration of the CO_2 plumes (for each interval), understanding the projected critical pressure fronts, and the pressure front decay and plume stabilization at post closure.

5.1 CRITICAL PRESSURE CALCULATIONS

The Cone of Influence (COI) is the area that surrounds the well where increased pressures due to injection operations can be sufficient to initiate vertical migration of fluids out of the injection zone through a potential conduit. The Cone of Influence is determined for each injection zone based upon the shallowest expected geologic depth to top of formation. This methodology used for calculating the cone of influence was developed by E. I. du Pont de Nemours & Co. (DuPont), and it is also generally consistent with previous methods (Barker, 1981; Clark et al., 1987; Collins, 1986; Davis, 1986; Johnson and Greene, 1979; Johnson and Knape, 1986; Warner, 1988; Warner and Syed, 1986).

The basic underlying assumption in this approach is that in the absence of naturally occurring, vertically transmissive conduits (faults and fractures) between the injection interval and any USDW, the only potential pathway between the injection zone and any USDW is through an artificial penetration (active or inactive oil and gas well(s)). In order to pose a potential threat to a USDW (*i.e.*, pressure buildup from injection sufficient to drive fluids into a USDW), the pressure increase in the injection interval would have to be greater than the pressure necessary to displace the material residing within the borehole. This pressure necessary to displace the material residing within the borehole is defined as the allowable buildup pressure. Therefore, the cone of influence is the area within which injection interval pressures are greater than the allowable buildup pressure.

5.2 AOR DELINEATIONS

The predicted AoRs (CO_2 plume and pressure front) are delineated based upon the reservoir modeling results using anticipated injection operation parameters [per 40 CFR 146.84(c)(1)(i)]. The pressure front, which proceeds the plume front, is delineated by using Cone of Influence designation and allowable pressure build-up in a borehole, which has been verified and used in multiple Class I application in the

Gulf Coast to evaluate the pressure fronts. The pressure front will be the expected maximum extent of the AoR, and therefore is used in the final AoR delineation. The cone of influence is the area within each injection interval, where pressures are greater than the allowable buildup pressure.

A static mud column exerts pressure. For an abandoned well to provide a pathway for fluid movement, the pressures acting on the static mud column (pressure due to injection plus original formation pressure) must be greater than the static mud column pressure. In a static fluid column, the gel strength of the mud must also be considered.

In this case, for upward fluid movement to begin, original formation pressure (P_f) plus the pressure due to injection (P_i) must be greater than the static fluid column pressure plus the gel strength of the mud. This relationship is based on a simple balance of forces (Davis, 1986):

$$P_f + P_i > P_s + P_g$$

Where:

P_f = original formation pressure (psig)

P_i = formation pressure increases due to injection (psi)

P_s = static fluid column pressure (psig)

P_g = gel strength pressure (psi)

Therefore, pressure increase due to injection must be greater than static fluid column pressure minus original formation pressure:

$$P_i > P_s + P_g - P_f$$

These relationships are used to determine the AOR and Cone of Influence for each of the injection intervals taking into consideration the dipping plane and redistribution of fluids within the reservoir during CO_2 injection. This study uses the predicted model pressure ($P_i + P_f$) at the end of the 20-year injection period, for each grid cell, in the top layer, minus the hydrostatic head (P_s) due to a 9.2-lb/gal column of "mud" at the same grid location to determine the AOR and Cone of Influence.

The cone of influence is the area where the pressure build-up due to injection is greater than the hydrostatic head of the mud column $(P_i + P_f) - Ps > 0$ (**Figure 39**). The AOR is defined as the point where the hydrostatic head pressure equals the pressure exerted by the column of mud (neglecting gel strength), $(P_i + P_f) - Ps = 0$.

The Cone of Influence and AOR are illustrated for the both the [redacted] Vernon site, and site to the southeast in the image below. **Appendix 8** provides detailed plots showing the AOR and Cone of influence for each injection interval.

6.0 CORRECTIVE ACTION PLAN

The potential for vertical movement through man-made breaches in the form of abandoned boreholes and active wells are addressed in this section. This corrective action evaluation assures that there will be no-migration of CO_2 and/or formation brine into an Underground Source of Drinking Water (USDW).

Whenever an effluent is injected into a subsurface geologic formation, the pressure within the injection sand(s) will increase. This pressure increase will be greatest at the injection well(s) and will decrease with distance away from the injection site. Because of the driving force supplied by the increase in formation pressure within the injection sand, artificial penetrations (legacy wells) within the radius of the CO_2 plume have the potential to convey CO_2 and formation fluids out of the injection zone, and artificial penetrations within the Area of Review have the potential to convey effluent into a USDW. In an unplugged borehole, this driving force is opposed by the flow resistance of the material (swelled clay, creeped shale, borehole collapsed material, in situ drilling mud) residing in the borehole. Vertical fluid movement out of the storage complex cannot begin until the pressure in the injection zone has increased beyond the critical threshold value necessary to overcome the flow resistance of the borehole material. If the pressure buildup in the injection sand is less than the threshold value, the artificial penetration cannot serve as a conduit for flow of formation brines out of the injection zone. Therefore, if the CO2 plume does not reach the artificial penetration, or the critical pressure for brine crossflow is not exceeded for a legacy well bore within the AoR, they have been evaluated as safe, and corrective action to plug the well is not necessary. After injection operations are completed, either temporarily or permanently, the pressure buildup within the injection sand will decrease to a value approaching the original formation pressure. This occurs rapidly, within a few years of cessation of injection. Upon pressure stabilization in the injection sand, the effluent plume will be in hydrostatic equilibrium with surrounding formation brines. Consequently, no driving force capable of conveying effluent or formation brines out of the injection zone will be present.

An Artificial Penetration Protocol is used to identify, locate, and evaluate artificial penetrations within the delineated AoR. A methodology for evaluating the construction or plugging of wells within the AoR was developed to evaluate a wells potential to act as a vertical conduit. Wells that are known to have been plugged across the injection interval, obviously cannot provide pathways for migration from the injection zone or injection-induced movement of fluids into a USDW, and do not require detailed evaluation. Wells that are plugged across the lowermost USDW, or at some point between the injection interval and the lowermost USDW, cannot serve as pathways for injection-induced movement of fluids into a USDW, but are evaluated as potential pathways for migration from the injection zone. Wells not known to have been plugged in either manner are further evaluated to determine whether they can serve as potential pathways for migration from the injection zone or for injection-induced movement of fluids into a USDW.

6.1 TABULATION OF WELLS WITHIN THE AOR

A thorough record search was conducted during preparation of this Vernon Parish - Class VI Well Application to locate and evaluate all wells that lie within the designated Area of Review. From the records obtained for each well in the AoR, a determination of penetration of the confining and injection zones was made. A total of 3 legacy wells have been located within the delineated AoR (See **Figure 2-22** in *"Project Information Tracking – Site Characterization"*) Complete tabulation data for all the wells located within the Area of Review are contained in **Table 35 [**per 40 CFR 146.82(a)(4)] and supporting documentation records for each well are presented in **Appendix 9.**

Table 35. List of wells within the AoR

[redacted]

6.1.1 Wells within the Area of Review Data Bases and Search Protocol

The AoR describes the area within which the owner or operator of a Class VI injection well must identify all artificial penetrations. These artificial penetrations could serve as potential conduits that would permit formation brine and or injected fluids to enter USDW and must be mitigated accordingly. This Artificial Penetration Protocol that follows consists of a program for well identification from various data sources, including file search at the LDNR Central File Room, as well as online public and commercial services.

6.1.1.1 Data Sources

Well location and completion data were acquired using IHS, SONRIS and LDNR resources. Wells were plotted using their reported surface locations and compared to the mapped area of interest surrounding the injection site. If discrepancies existed among data sources, the reported state data was considered to be the most accurate. If data were not available, hardcopy searches were performed to complement the search. The following discussion provides a synopsis of the procedures used to procure this state data.

Wells that were in the AOR were identified. This resulted in the identification of 3 wells.. Each well was then investigated regarding its total depth based on completion reports and well logs. It was determined that all five wells penetrate the primary confining unit for the Vernon One GS site. Upon further investigation it was determined that three of the five wells within the AoR are to be replugged prior to injection.

6.1.1.2 Search Protocol

To begin research of non-freshwater artificial penetrations in the AoR, the search first obtains base maps available from commercial mapping companies and from SONRIS. These base maps are used to determine the well locations and land survey grids such as townships, ranges, and sections. A larger AoI (all wells within a 3-mile radius of the injection site) was then defined, over potentially affected areas. The larger initial search footprint provides a due diligence of wells that may be near or surrounding the outside perimeter of the finalized AoR.

The LDNR, Office of Conservation, is the state oil and gas regulatory authority and repository for records of all oil and gas wells drilled in the state and is considered the most reliable source of oil and gas data in Louisiana. This agency can usually provide 95 to 100 percent of the data needed, along with the online resources and the available hardcopies in the central file room.

The Louisiana well serial number is the most important reference for accessing the well record file through the LDNR Office of Conservation Well File Department. The well serial number system is very efficient in the state of Louisiana. The system was implemented at the time of the origin of the agency and has remained intact since. When an oil and gas operator acquire a permit to drill in Louisiana, the proposed well is assigned a permanent serial number. Subsequently, any completion, plug back, deepening, or plugging reports are filed under this serial number regardless of any changes in operator ownership or lease name.

As an additional backup used in verifying wells drilled, the Office of Conservation has a computer database titled "SONRIS." This database allows the researcher to input the township, range, and section of interest to receive a complete printout of all serial numbers permitted in that area. In addition, the SONRIS database has an interactive Public GIS Map, that a user may use by creating a search box / polygon around an area of interest, to also investigate records and data available for the wells. These databases are available to confirm well depth, status (expired permit, producing, or plugged), and current operator. These database

programs provide additional support to ensure that data on the field map maintained by the Office of Conservation are accurate.

Occasionally, there are instances in which well records are not located in the well file system of the Department of Conservation's office in Baton Rouge, Louisiana. In such cases, it is necessary to check the appropriate district office. Although the district offices primarily retain only more current data, some older data are available. These well records are also filed by the well's serial number. District office personnel are sometimes able to provide other potential sources for information not available at the district office.

> **Louisiana Geological Survey:** This agency contains a library of geological reports, which, in some cases, provide information pertaining to a missing well. There also may be information relevant to the completion and plugging methods utilized in specific areas and/or during time periods. The Geological Survey can also provide recommendations of little known or underutilized sources of information.
>
> **Commercial Log Libraries:** When required data cannot be obtained from either the Louisiana Department of Natural Resources or the Louisiana Geological Survey, data can be acquired using membership privileges with a commercial geologic and well log library. These libraries maintain extensive electric log collections as well as scout ticket files. Scout tickets often prove very valuable since full operator name or alternative operator names are listed. These alternative operator names often allow researchers to re-enter the Office of Conservation's filing system with previously unknown record leads. Note: that as this data is commercially provided through a membership, data is considered CBI.

For the Vernon One site, the well location and completion data were acquired using IHS, SONRIS and LDNR resources. Data for all wells within the final determine AoR was available. A hard copy search of the Microfilm/Microfiche at the LDNR Baton Rouge office was also performed in February 2023 to verify all data had available had been acquired.

The search resulted in the identification of three wells within the delineated AoR. Each well was then investigated regarding its total depth based on completion reports and well logs. It was determined that all three wells penetrate the primary confining unit for the Vernon One site. As a result, CapturePoint has determined that all three wells within the AoR will be re-plugged prior to authorization to inject.

6.1.2 **Well Evaluation**

Each artificial penetration (active/abandoned) was evaluated as to the adequacy of construction and plugging to determine the potential of the penetration to convey fluid from an injection zone into the overlying USDWs (non-endangerment) and the potential of the penetration to convey injected effluent out of the injection zone (no migration) [40 CFR 146.84 (c)(3)].

For the purpose of the evaluation, a properly constructed active well (producing, injecting, shut-in, temporarily abandoned, *etc.)* is defined as a well in which the surface casing has been set through all USDWs. These wells are constructed to standards for protecting freshwater aquifers. Active wells with "short" surface casing that does not extend below all USDWs potentially present a conduit outside of the protection and/or production casing, or open hole, into USDWs. These wells are labeled as "potential problem wells" and are further evaluated or modeled for potential upward movement of fluids. Although the drilling fluid in the annulus would provide the same resistance to vertical fluid movement as a mud plug in an open wellbore, active wells that were constructed improperly were also listed as potential problem wells and evaluated or modeled for possible vertical fluid movement.

Cement volume calculations were made on each well that has full protection and/or production casing left intact in the well. Only conservative data values were used in the calculations. Additionally, a 35 percent

additional slurry volume requirement was calculated in the cased and open hole wellbores. Cement slurry volumes were calculated using a combined 75 percent lead cement (1.913 ft^3/sack-slurry volume) and a 25 percent tail Class H cement (1.179 ft^3/sack-slurry volume). This is a very typical design for casing and cementing programs.

One well, William Burton #2 only showed a partial plugging record found. Currently, the LA DNR District Office in Lafayette is closed for maintenance. All hard copy records are being stored off site and unavailable for use. Once the District office is re-opened with access to the records, it is believed we will find additional detail and evaluation material and the recommended action may change. Two wells, the Crosby Chemicals #1 and Indigo 25H were found to be properly plugged and require no action. The Crosby Chemicals #1 well had 13-3/8" surface casing ran to 4,000'. Cement is considered circulated to surface because the LA DNR requires this on all surface casing. Additionally, the conservative cement calculations were considered and indicate cement would be circulated.

6.1.3 Wells Penetrating the Confining Zone

Wells that penetrate the confining and/or injection zone may have the potential for conveying fluid from the injection zone to an overlying formation or from the injection zone to an overlying USDW. Wells that penetrate the Confining Zone are included in all pressure and plume front evaluations per 40 CFR 146.84(c)(2). Available geophysical well logs from the artificial penetrations within the AoR were evaluated to determine which of the wells penetrate the confining/injection zone. Wells that do not penetrate the primary confining zone ([redacted]) do not provide potential avenues for fluid movement and need not be evaluated further.

A properly plugged well that penetrates the confining zone (and the deeper injection zones), will have at minimum of a plug set across the base of the primary/[redacted] or secondary/ J[redacted] confining zone. Plugging materials in artificial penetrations will be evaluated to determine if they are compatible with the CO_2 stream [40 CFR 146.84(d)].

Within the AoR there are five wells that penetrate the primary confining unit, of these, two wells require no additional corrective action. The remaining three wells including the William Burton #2 above were identified to require re-plugging. These wells are plugged and abandoned oil and gas exploration wells that were drilled in the 1970 and 1980's. These wells were plugged according to regulatory standards of that time. As a result, these wells will require CapturePoint Solutions, LLC to replug these wells according to current regulatory plugging requirements using the necessary materials with respect to potential exposure to CO_2 and affected formation fluids. The replugging of these wells will occur prior to the start of injection operations at the Vernon One CCS Site.

6.2 PLAN FOR SITE ACCESS

Surface Use and Access Agreements for the Vernon One CCS Site will be established with landowners. This will ensure that CPS will have complete access for all phases of the project in order to perform corrective action, conduct site monitoring and site care and site closure operations.

6.3 CORRECTIVE ACTION SCHEDULE

Schematics and records data (well log headers, well Plats, APD files, plugging reports and deviation surveys) for all of the artificial penetrations within the delineated AoR are included in **Appendix 9**.

Information included on the well schematics are: permit application identification number; operator information; well lease name; status; casing information; key regulatory datums; and cement type and plugging depths.

For purposes of evaluating artificial penetrations, conservative construction and/or plugging conditions were used to determine proper plugging requirements for the protocol. The evaluation protocol requires that all formations bearing USDWs, oil, gas or geothermal resources be protected with type-specific cement plugs and mud-laden fluid. Setting depths for cement plugs are dependent upon the construction of the well and the geological environment.

Wells abandoned with only surface casing set through all USDWs should be plugged across the base of the lowermost USDW regardless of casing depth. When insufficient surface casing is set to protect all USDWs and such strata are exposed to the open wellbore, a cement plug must be installed. When sufficient surface casing has been set to protect all USDWs, a cement plug must be set across the surface casing shoe.

For wells abandoned with surface casing set through all USDWs and with protection and/or production casing that has been cemented upwards through the lowermost USDW (or to surface), these wells contain a "double-seal", ensuring that USDWs are protected. Wells that contain "short" surface casings that are set above the lowermost USDW and within which the protection and/or production casing that has not been cemented upwards through the lowermost USDW (or to surface) are determined to be improperly plugged by the above criteria. These wells potentially present a conduit outside of the protection and/or production casing into USDWs. These wells are labeled as "potential problem wells" and are further evaluated or modeled for potential upward movement of fluids.

Three of the five wells within the AoR that were drilled, plugged, and abandoned in the AoR area will require a corrective action plan to protect all USDWs. All wells will be re-plugged before CO_2 injection begins in the reservoir. The cement(s) formulated for re-plugging will be designed to prevent any unwanted fluid movement, resist the corrosive aspects of CO_2 with water mixtures and protect all USDWs. In the open hole intervals, the cement volume will include 35 percent excess. In summary, cement plug #1 will be set with a bottom approximately 100 feet into the proposed [redacted] injection zone or approximately 100 feet below the base of the [redacted], the top confining zone, and with a cement plug top approximately 500 feet into the [redacted] confining zone. Cement plug #2 will be set approximately 100 feet below the Base of the [redacted] confining zone with a top approximately 500 feet into the [redacted] confining zone. Plug #3 will be set approximately 300 feet below the lowest known USDW depth with additional plugs layered to surface. The casing will be cut off 5 feet below the ground and a metal plate installed on the casing with the required information attached. Additional details on each re-plug follows below.

CapturePoint Solution, LLC will notify the regulatory agency, as required, before re-plugging the wells and provide updated plans, if applicable.

6.3.2 Well 1 – Bentley Lumber Co. No 6 – Corrective Action Plan

Proposed Re-Plug Procedure for Bentley Lumber Co. No 6

Figure 40 is the current plug and abandon wellbore diagram. **Figure 41** is the proposed re-plug and abandon wellbore diagram. **Table 36** is a summary of the proposed cement plug depths, properties, and volumes.

1. Dig cellar and find casing the weld on plate and well information.
2. Hot tap well plate and install pressure gauge to confirm no pressure or gas at surface.
3. Install wellhead and nipple up BOP (blowout preventer).
4. Mix workover fluid, estimated to be 9.8 ppg but adjusted as needed.
5. Pick up bit and work string. Clean out 10 sack cement plug at surface to an estimated 30'.
6. Run in the hole and tag 35 sack cement plug #2 at 600'. Drill down to 700'. Circulate clean.
7. Run in hole and tag 70 sack cement plug #3 at 1,065'. Drill to bottom of plug at 1,275'. Circulate clean.
8. Run in hole to 3,650'. Circulate hole clean. Prior to setting plugs, the well shall be in a state of equilibrium with the weight of the workover fluid equalized from top to bottom. This workover fluid, estimated to be 9.7 ppg, will be used to displace cement and will remain between plugs where required.
9. Mix 218 sacks of CO2 resistant cement. Spot 600' balanced plug #1 from a bottom of 3,650' to a top at 3,050'. The bottom of the plug will be approximately 93' into the [redacted] injection zone and approximately 93' below the base of the top confining zone in the [redacted]. The top of plug will be set approximately 507' into the [redacted] confining zone. Displace cement with workover fluid. Allow cement to set then tag top of plug.
10. Pick up tubing to 2,600'. Mix 218 sacks of CO2 resistant cement. Spot 600' balanced plug #2 from a bottom of 2,600 to a top of 2,000'. The bottom of the plug will be approximately 261' below the base of the J[redacted] confining zone. The top of the plug will be approximately 339' into the [redacted] confining zone. Displace cement with workover fluid. Allow cement to set, then tag top of plug.
11. Pick up tubing to 1,850'. Mix 233 sacks of Class H cement plus additives. Spot 600' balanced plug #3 from a bottom of 1,850' to a top of 1,250'. The bottom of the plug will be approximately 301' below the base of the USDW. Displace cement with workover fluid. Allow cement to set, then tag top of plug at 1,250'.
12. Mix 237 sacks of Class H cement plus additives. Spot 600' balanced plug #4 from a bottom of 1,250' to a top of 650'. Displace cement with workover fluid. The bottom plug will be 435' below surface casing @815' and 165' inside the 8-5/8" casing. Allow cement to set, then tag top of plug at 650'.
13. Mix 196 sacks of Class H cement plus additives. Spot 645' balanced plug #5 from 650' to 5' below surface. Allow cement to set.
14. Cut casing 5' below ground level. Clean cellar and weld on plate with required well information. Backfill wellhead and clean location.

Figure 40. Existing plugs for well Bentley Lumber Co. No 6

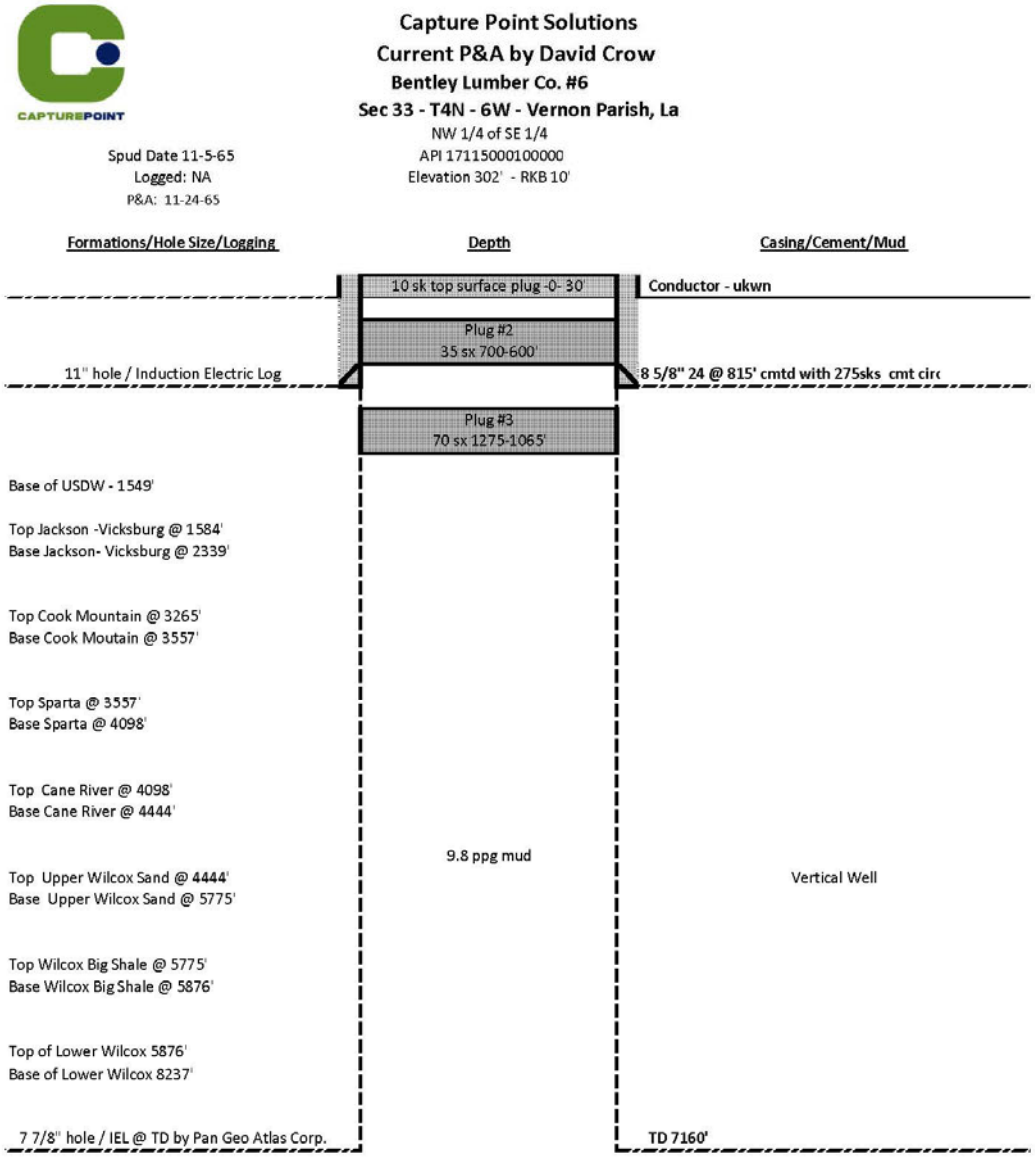

Figure 41. Proposed plugging plan for well Bentley Lumber Co. No 6

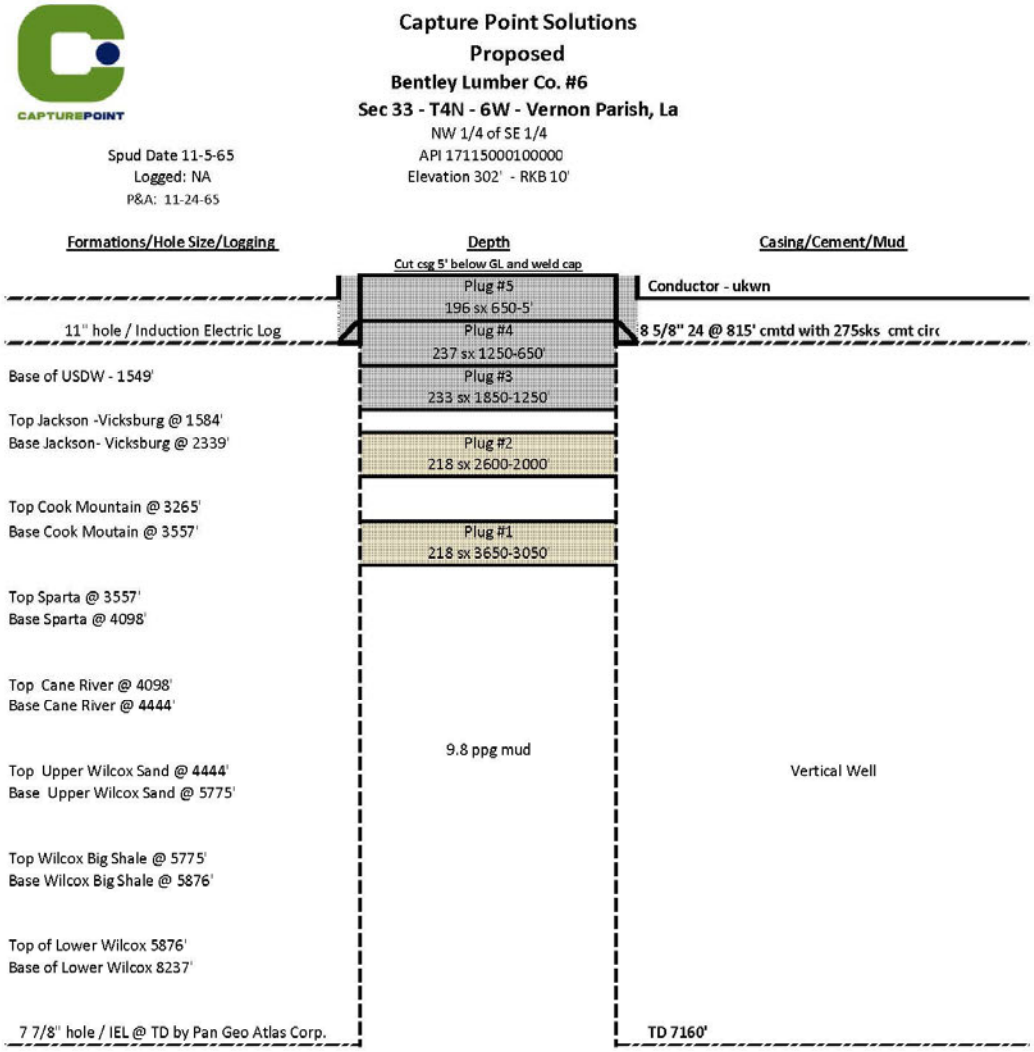
Capture Point Solutions
Proposed
Bentley Lumber Co. #6
Sec 33 - T4N - 6W - Vernon Parish, La
NW 1/4 of SE 1/4
API 17115000100000
Elevation 302' - RKB 10'
Spud Date 11-5-65
Logged: NA
P&A: 11-24-65
Formations/Hole Size/Logging
Depth
Cut csg 5' below GL and weld cap
Casing/Cement/Mud
Plug #5
196 sx 650-5'
Conductor - ukwn
11" hole / Induction Electric Log
Plug #4
237 sx 1250-650'
8 5/8" 24 @ 815' cmtd with 275sks cmt circ
Base of USDW - 1549'
Plug #3
233 sx 1850-1250'
Top Jackson -Vicksburg @ 1584'
Base Jackson- Vicksburg @ 2339'
Plug #2
218 sx 2600-2000'
Top Cook Mountain @ 3265'
Base Cook Moutain @ 3557'
Plug #1
218 sx 3650-3050'
Top Sparta @ 3557'
Base Sparta @ 4098'
Top Cane River @ 4098'
Base Cane River @ 4444'
9.8 ppg mud
Top Upper Wilcox Sand @ 4444'
Base Upper Wilcox Sand @ 5775'
Vertical Well
Top Wilcox Big Shale @ 5775'
Base Wilcox Big Shale @ 5876'
Top of Lower Wilcox 5876'
Base of Lower Wilcox 8237'
7 7/8" hole / IEL @ TD by Pan Geo Atlas Corp.
TD 7160'

Table 36 – Bentley Lumber Co. No 6 – Proposed Cementing Details

Plug Information	Plug #1	Plug #2	Plug #3	Plug #4	Plug #5
Diameter of casing in which plug will be placed (Inches)	7.875	7.875	7.875	7.875 Open Hole and 8.097	8.097
Depth to bottom of tubing (Feet)	3,650	2,600	1,850	1,250	650
Sacks of Cement to be used (each plug)	218	218	233	237	196
Slurry volume to be pumped (ft3)	274	274	274	279	231
Slurry weight (lb/gal)	14.5	14.5	15.6	15.6	15.6
Calculated top of plug (ft)	3,050	2,000	1,250	650	5
Bottom of plug (ft)	3,650	2,600	1,850	1,250	650
Type of cement or other material	CO2 resistant cement	CO2 resistant cement	Cl H plus additives	Cl H plus additives	Cl H plus additives
Method of emplacement (e.g., balance method, retainer method, or two-plug method)	Balance Plug	Balance Plug	Balance Plug	Balance Plug	Balance Plug

6.3.4 Well 2 – Pardee No 2 – Corrective Action Plan

Proposed Re-Plug Procedure for Pardee No 2

Figure 42 is the current plug and abandon wellbore diagram. **Figure 43** is the proposed re-plug and abandon wellbore diagram. **Table 37** is a summary of the proposed plug depths, slurries, properties, and volumes of cement plugs required.

1. Dig cellar and find casing with weld on plate and well information.
2. Tap well plate and install pressure gauge to confirm no pressure or gas at surface.
3. Install wellhead and nipple up BOP (blowout preventer).
4. Mix workover fluid, estimated to be 9.5 ppg but adjusted as needed.
5. Pick up bit and work string. Clean out 15 sack cement plug at surface to an estimated 30'.
6. Run in the hole and tag 35 sack cement plug #2 at 1,352'. Drill down to 1,452'. Circulate clean.
7. Run in hole and tag 35 sack cement plug #3 at 1,710'. Drill to bottom of plug at 1,810'. Circulate clean.
8. Run in hole to 4,110'. Circulate hole clean. Prior to setting plugs, the well shall be in a state of equilibrium with the weight of the workover fluid equalized from top to bottom. This workover fluid, estimated to be 9.5 ppg, will be used to displace cement and will remain between plugs where required.
9. Mix 218 sacks of CO2 resistant cement. Spot 600' balanced plug #1 from a bottom of 4,110' to a top at 3,510'. The bottom of the plug will be approximately 100' into the [redacted] injection zone and approximately 100' below the base of the top confining zone in the [redacted]. The top of plug will be set approximately 500' into the [redacted] confining zone. Displace cement with workover fluid. Allow cement to set then tag top of plug.
10. Pick up tubing to 3,079'. Mix 218 sacks of CO2 resistant cement. Spot 600' balanced plug #2 from a bottom of 3,079 to a top of 2,479'. The bottom of the plug will be approximately 300' below the base of the [redacted] confining zone. The top of the plug will be approximately 300' into the [redacted] confining zone. Displace cement with workover fluid. Allow cement to set, then tag top of plug.
11. Pick up tubing to 2,180'. Mix 233 sacks of Class H cement plus additives. Spot 600' balanced plug #3 from a bottom of 2,180' to a top of 1,580'. The bottom of the plug will be approximately 300'' below the base of the USDW. Displace cement with workover fluid. Allow cement to set, then tag top of plug at 1,580'.
12. Mix 242 sacks of Class H cement plus additives. Spot 600' balanced plug #4 from a bottom of 1,580' to a top of 980'. Displace cement with workover fluid. Allow cement to set, then tag top of plug at 980'. The bottom plug will be approximately 178' into openhole and top of plug will be approximately 422' into surface casing.
13. Mix 246 sacks of Class H cement plus additives. Spot 600' balanced plug #5 from a bottom of 980' to a top of 380'.
14. Mix 114 sacks of Class H cement plus additives. Spot 375' balanced plug #6 from 380' to 5' below surface. Allow cement to set.
15. Cut casing 5' below ground level. Clean cellar and weld on plate with required well information. Backfill wellhead and clean location.

Figure 42. Existing plugs for well Pardee No 2

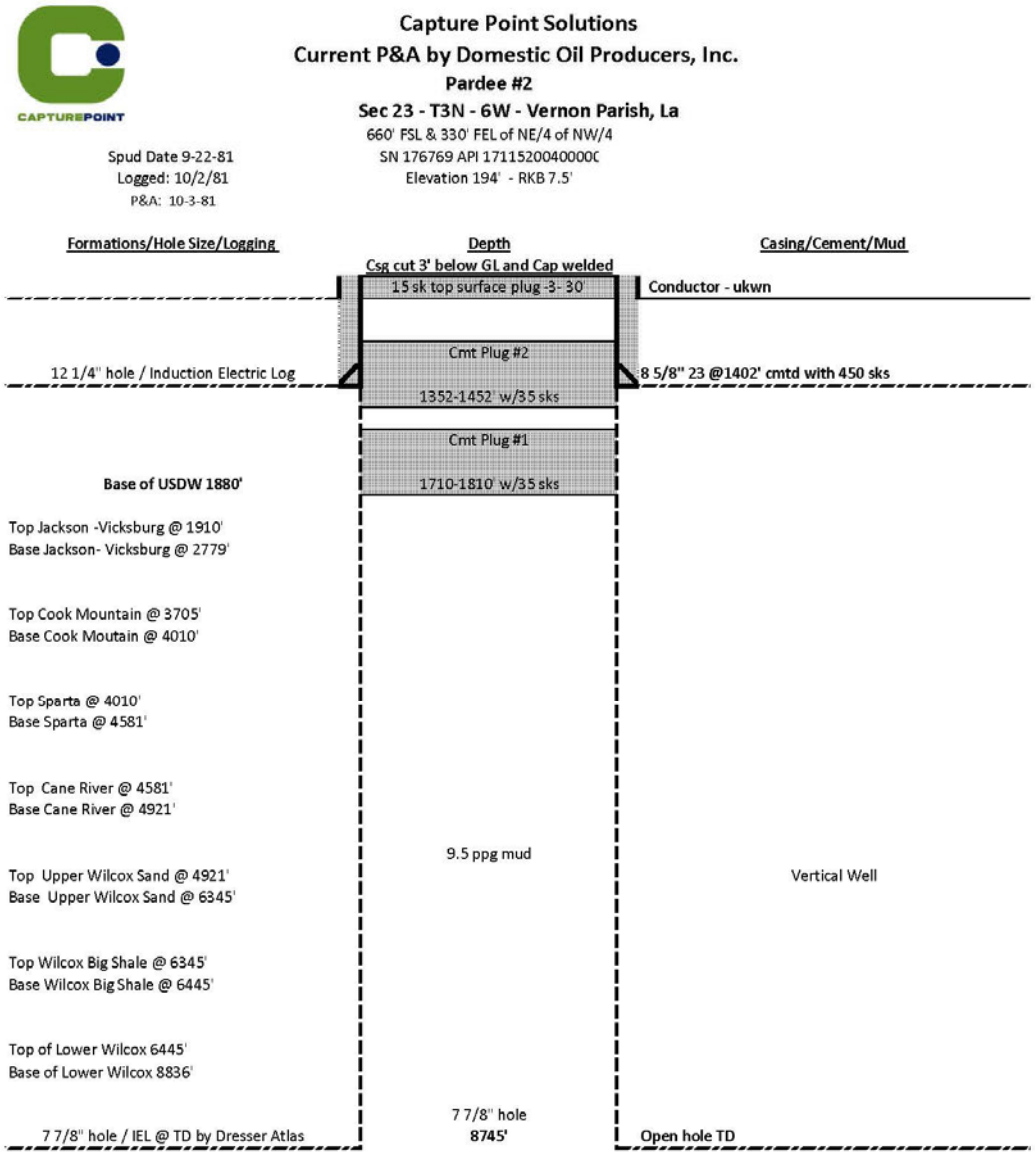

Figure 43. Proposed plugging plan for well Pardee No 2

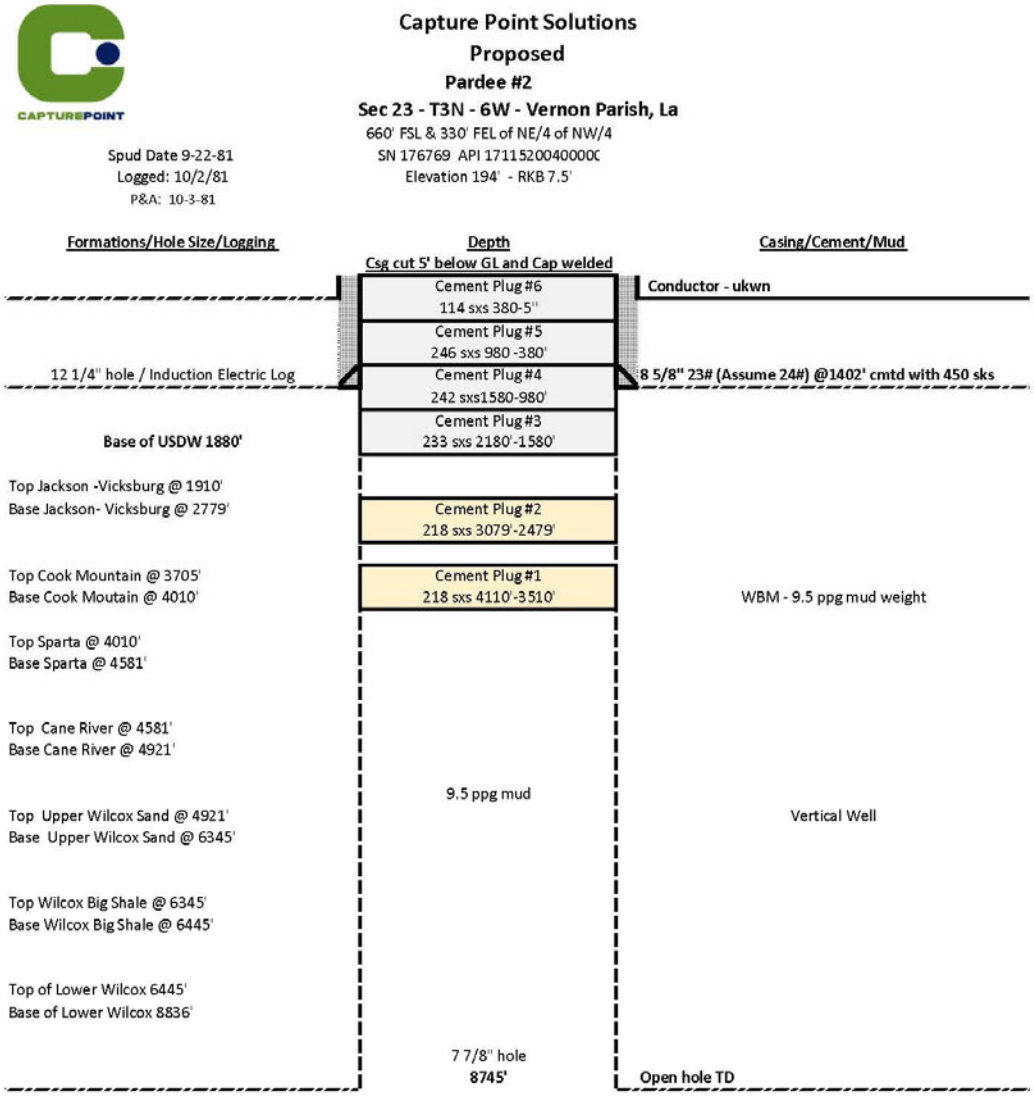

Table 37 – Pardee No 2 – Proposed Cementing Details

Plug Information	**Plug #1**	**Plug #2**	**Plug #3**	**Plug #4**	**Plug #5**	**Plug #6**
Diameter of casing in which plug will be placed (Inches)	7.875	7.875	7.875	7.625 Open Hole and 8.097	8.097	8.097
Depth to bottom of tubing (Feet)	4,110	3,079	2,180	1,580	980	380
Sacks of Cement to be used (each plug)	218	218	233	242	246	114
Slurry volume to be pumped (ft3)	274	274	274	285	290	135
Slurry weight (lb/gal)	14.5	14.5	15.6	15.6	15.6	15.6
Calculated top of plug (ft)	3,510	2,479	1,580	980	380	5
Bottom of plug (ft)	4,110	3,079	2,180	1,580	980	380
Type of cement or other material	CO2 resistant cement	CO2 resistant cement	Cl H plus additives	Cl H plus additives	Cl H plus additives	Cl H plus additives
Method of emplacement (e.g., balance method, retainer method, or two-plug method)	Balance Plug	Balance Plug	Balance Plug	Balance Plug	Balance Plug	Balance Plug

6.3.6 Well 3 – William Burton No 2 – Corrective Action Plan

Proposed Re-Plug Procedure for Pickering William Burton No 2

Figure 44 is the current plug and abandon wellbore diagram. **Figure 45** is the proposed re-plug and abandon wellbore diagram. **Table 38** is a summary of the proposed plug depths, slurries, properties, and volumes of cement plugs required.

1. Dig cellar and find casing with weld on plate and well information.
2. Tap well plate and install pressure gauge to confirm no pressure or gas at surface.
3. Install wellhead and nipple up BOP (blowout preventer).
4. Mix workover fluid, estimated to be 9.5 ppg but adjusted as needed.
5. Pick up bit and work string. RIH to 4,623'. Circulate hole clean. Prior to setting plugs, the well shall be in a state of equilibrium with the weight of the workover fluid equalized from top to bottom. This workover fluid, estimated to be 9.5 ppg, will be used to displace cement and will remain between plugs where required. POOH with work string.
6. Perforate squeeze perfs at 4,623'. RIH with pkr. Set pkr @ 3700'.
7. Mix 183 sacks of Class H cement with additives. Squeeze 50 sacks into perfs at 4,623' and Spot 600' balanced plug #3 from a bottom of 4623' to a top at 4,023'. The bottom of the plug will be approximately 62' into the top confining zone in the [redacted] and 300' below the surface casing shoe. The top of plug will be set approximately 300' into the surface casing. Displace cement with workover fluid. Allow cement to set then tag top of plug.
8. Pick up work string to 100'. Mix 13 sacks of Class H cement plus additives. Spot 100' surface balanced plug #4 from 100' to 5' below surface. Allow cement to set.
9. Cut casing 5' below ground level. Clean cellar and weld on plate with required well information. Backfill wellhead and clean location.

Figure 44. Existing plugs for well William Burton No 2

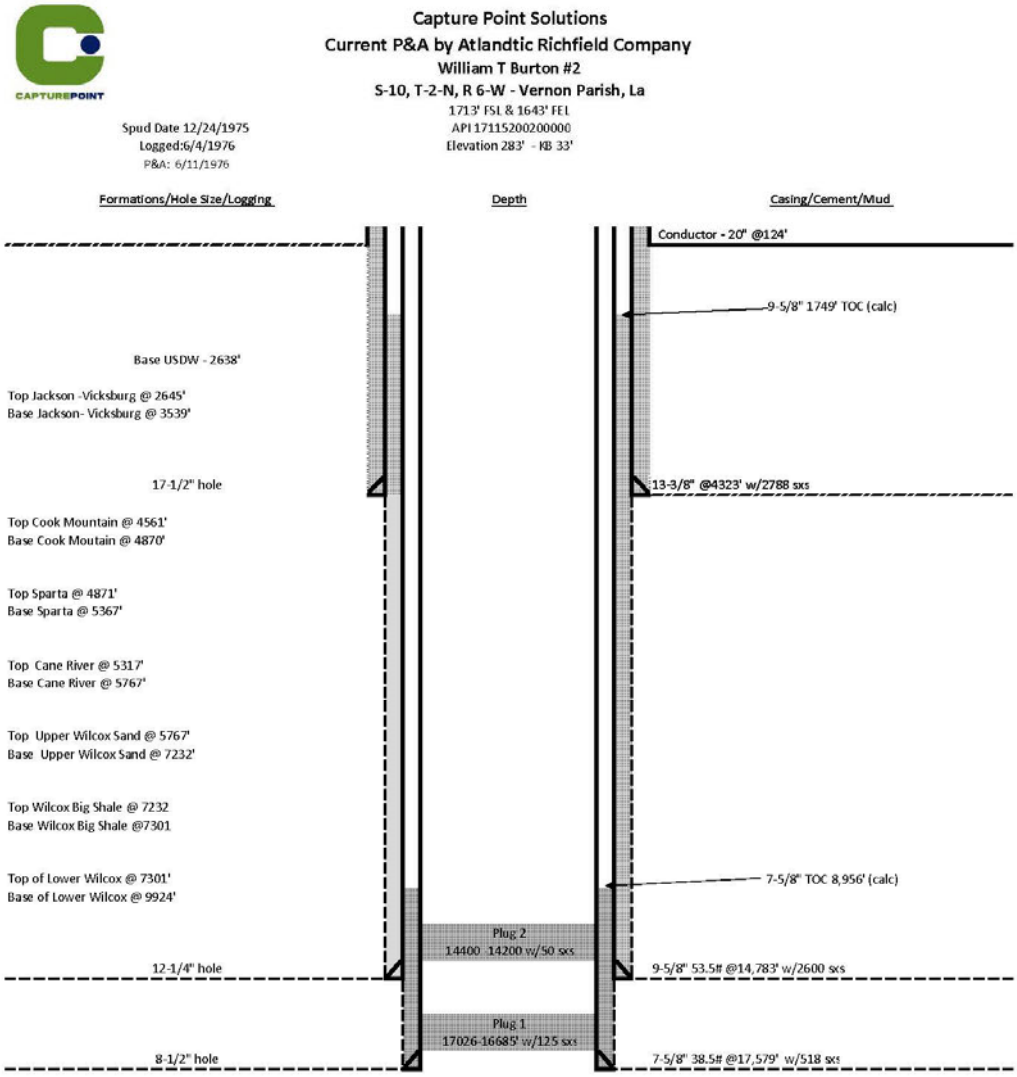

Figure 45. Proposed plugging plan for well William Burton No 2

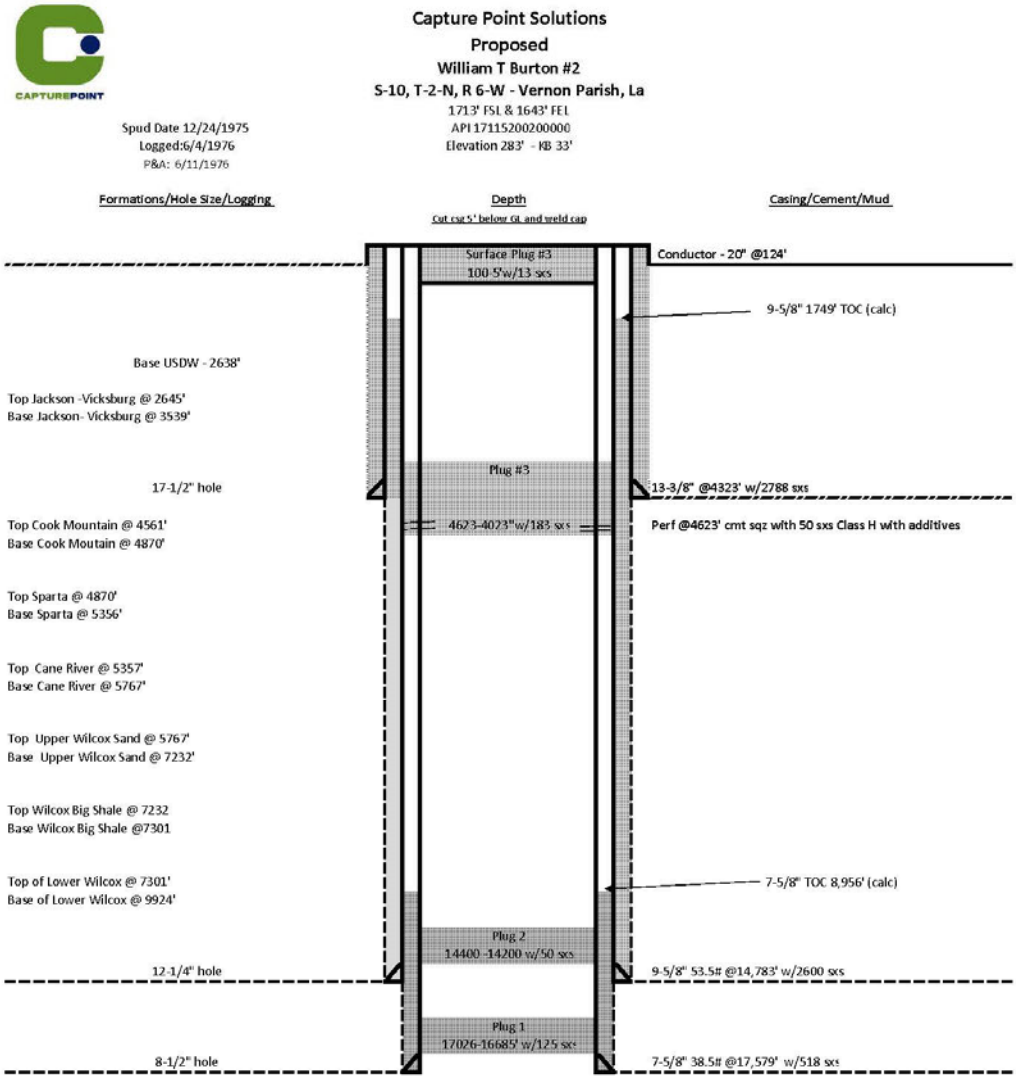

Table 38 – William Burton No 2 – Proposed Cementing Details

Plug Information	**Plug #3**	**Plug #4**
Diameter of casing in which plug will be placed (Inches)	6.765	6.765
Depth to bottom of tubing (Feet)	4623	100
Sacks of Cement to be used (each plug)	183	13
Slurry volume to be pumped (ft3)	126	14.2
Slurry weight (lb/gal)	15.6	15.6
Calculated top of plug (ft)	4023	5
Bottom of plug (ft)	4623	100
Type of cement or other material	Cl H plus additives	Cl H plus additives
Method of emplacement (e.g., balance method, retainer method, or two-plug method)	Sqz 50 sxs plus Balance Plug	Balance Plug

6.3.7 Well 4 – Crosby Chemicals No 1 – Corrective Action Plan

No Action Required. The Current P&A is adequate to protect the USDW.

Figure 46. Existing plugs for well Crosby Chemicals No 1

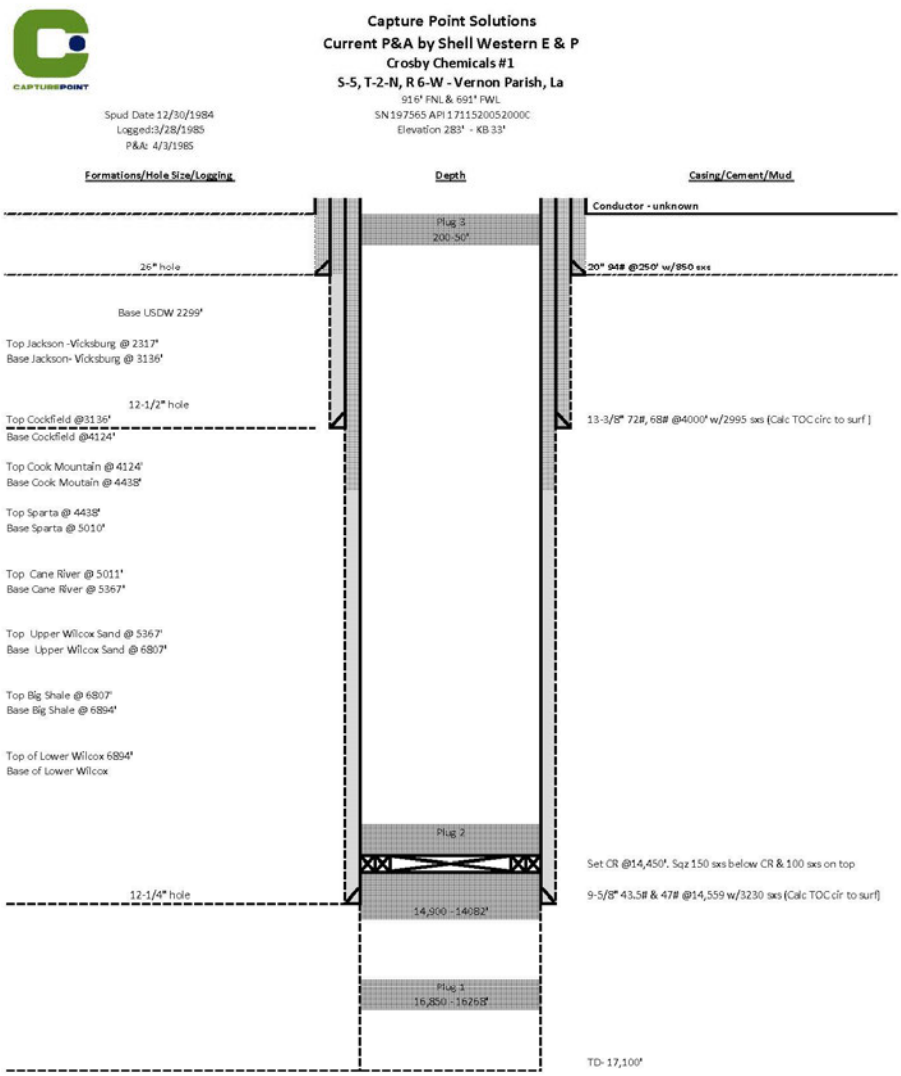

6.3.8 Well 8 – Indigo 25 H – Corrective Action Plan

No Action Required. The Current P&A is adequate to protect the USDW.

Figure 47. Existing plugs for well Indigo 25 H

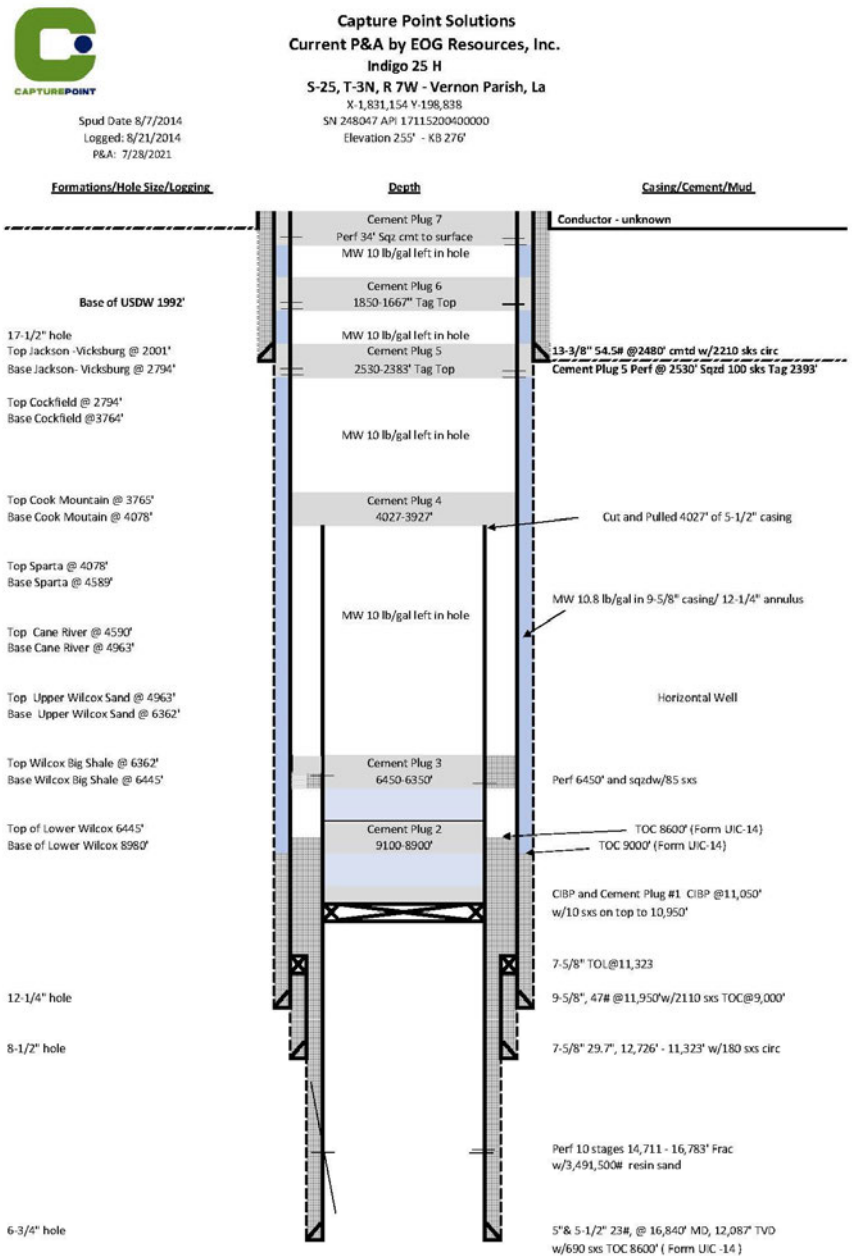

7.0 RE-EVALUATION SCHEDULE AND CRITERIA

7.1 AoR Re-evaluation Cycle

CapturePoint, LLC will reevaluate the above described AoR will be reevaluated at least once every 5-years during the injection and post-injection phases [40 CFR 146.84(e)]. Additionally, testing and monitoring of the site contains benchmarks/milestones that may trigger AoR reevaluations more often.

Testing and Monitoring data, will be collected annually. Injection operations will be monitored at their set frequency. All data will be compiled and reviewed and then compared alongside the corresponding calculated output from the simulation model. The data will include (at a minimum):

1) Injection mass rates per day, volume rates, tubing head pressures and temperatures per each well.

2) Downhole pressures and temperatures daily per well.

3) Where available, wireline logs of CO_2 injection rates per zone.

4) Pressure fall-off data, where available, per well.

5) In zone and above zone pressure data from monitoring wells.

The model will be updated with actual daily CO_2 injection volumes for each well. The simulation model will be history matched to be representative of current conditions and then projected forward. Pressures will be monitored as presented in "*Testing and Monitoring Plan*" submitted in Module E – Project Plan Submissions. Time-lapse pressure profiled will be compared between actuals and predicted pressure profiles.

If a new AoR is delineated that will include additional Artificial Penetrations, these additional wells will be revaluated. These wells will be evaluated for status, construction and plugging details, location, depth of penetration, and verify that each new well meets the standard to prevent the movement of CO_2 or other fluids out of the injection zone or endanger a lowermost USDW. If a well fails the evaluation criteria, the corrective action plan will be revised to include a deficient well.

7.2 Triggers for AoR Reevaluations Prior to the Next Scheduled Reevaluation

Unscheduled AoR reevaluations may occur if unexpected changes are detected in the monitoring of the Vernon Parish injection site. Unexpected changes may be represented by fluctuations in pressure, temperature, water analysis, or major variations from modeled front behaviors. Examples that may trigger an earlier AoR reevaluation are as follows:

1. Increases in downhole pressures that exceed the model simulation and have an impact on the formation injectivity.
2. Increases in pressures in the above confining zone monitoring well which could indicate leakage above the formation.
3. A large decrease in expected formation pressures, which could indicate a leak.
4. An increase in CO_2 measured at surface.
5. Continuous monitoring systems determine that an injection operating parameter has been exceeded (such as total volume).
6. Additional site characterization information that will provide additional information.

7. Arrival times of Pressure/Plume fronts vary in the in-zone monitoring well from modeled timeframes.
8. If at any time, the pressures in the monitoring wells exceeds fracture gradient limits.

Details of events that may trigger a reevaluation based upon monitoring parameters are contained in the "*Testing and Monitoring Plan*" submitted in Module E – Project Plan Submissions.

CapturePoint, LLC will discuss any such events with the UIC Program Director to determine if an AoR reevaluation is required. If an unscheduled reevaluation is triggered, CapturePoint, LLC will perform the steps described at the beginning of this section of this Plan

8.0 REFERENCES:

Amyx, J. W., Bass D. M., and Whiting, R. L., 1960, Petroleum Reservoir Engineering: McGraw-Hill Book Company, New York, New York, p. 63.

Barker, S. E., 1981, Determining the Area of Review for Industrial Waste Disposal Wells: Master's Thesis, The University of Texas at Austin, Austin, Texas, 146 p.

Celia, M.A. and Nordbotten, J.M., 2009, Practical Modeling Approaches for Geological Storage of Carbon Dioxide, in press, Ground Water.

Clark, J. E., Howard, M. R., and Sparks, D. K., 1987, Factors that can cause abandoned wells to leak as verified by case histories from Class II injection, Texas Railroad Commission Files: International Symposium on Subsurface Injection of Oil Field Brines, Underground Injection Practices Council, New Orleans, Louisiana, p. 166-223.

Collins, R. E., 1986, Technical basis for area of review, an engineering study prepared for Chemical Manufacturers Association: Chemical Manufacturers Association Reference Number 80-160-000-4.

Collins, R. E. and Kortum, D., 1989, Drilling mud as a hydraulic seal in abandoned wellbores: Underground Injection Practices Council, 1989 Winter Meeting, San Antonio, Texas.

Davis, K. E., 1986, Factors effecting the area of review for hazardous waste disposal wells: Proceedings of the International Symposium on Subsurface Injection of Liquid Wastes, New Orleans, National Water Well Association, Dublin, Ohio, p. 148-194.

Eaton, B. A., 1969, Fracture gradient prediction and its application in oilfield operations: Transactions of the American Institute of Mechanical Engineers, v. 246

Fetter, C. W., 1988, Applied Hydrogeology: Merrill Publishing Company, Columbus, Ohio, 592 p.

Johnston, O. C. and Greene, C. J., 1979, Investigation of artificial penetrations in the vicinity of subsurface disposal wells-Technical Report: Texas Department of Water Resources.

Johnston, O. C., and Knape, B. K., 1986, Pressure Effects of the Static Mud Column in Abandoned Wells: Texas Water Commission LP 86-06, 106 p.

Kasmarek, M. C., 2012, Hydrogeology and simulation of groundwater flow and land-surface subsidence in the northern part of the Gulf Coast Aquifer System, Texas, 1891-2009: U.S. Geological Survey Scientific Investigations Report 2012-5154, 55 p.

Kasmarek, M. C., Gabrysch, R. K., and Johnson, M. R., 2010, Estimated land-surface subsidence in Harris County, Texas, 1915–17 to 2001: U.S. Geological Survey Scientific Investigations Map 3097.

Kasmarek, M. C., and Ramage, J. K., 2017, Water-Level Altitudes 2017 and Water-Level Changes in the Chicot, Evangeline, and Jasper Aquifers and Compaction 1973–2016 in the Chicot and Evangeline Aquifers, Houston-Galveston Region, Texas: U.S. Geological Survey Scientific Investigations Report 2017-5080, 32 p.

Laesecke, A. and Muzny, C.D., 2017, Reference Correlation for the Viscosity of Carbon Dioxide, Journal of Physical and Chemical Reference Data, Volume 46, Issue 1

Lohrenz, J., Bray, B.G., and Clark, C.R., 1964, Calculating Viscosities of Reservoir Fluids from Their Compositions, Journal of Petroleum Technology, 1171 Trans, AIME 231.

Moore, P. L., 1974, Drilling Practices Manual: PennWell Books, Tulsa, Oklahoma.

Newman, G. H., 1973, Pore-volume compressibility of consolidated, friable, and unconsolidated reservoir rocks under hydrostatic loading: Journal of Petroleum Technology, p. 129-134.

Peng, D.Y. and Robinson, D.B., 1978, The Characterization of the Heptanes and Heavier Fractions for the GPA Peng-Robinson Programs. Research report (Gas Processors Association). Gas Processors Association.

Porter, W. M. and Newsom, S. W., 1987, Shale Porosity and Permeability: DuPont Report.

Wang, Y., Vuik, C., and Hajibeyji, H., 2022, Analysis of hydrodynamic trapping interactions during full-cycle injection and migration of CO2 in deep saline aquifers, Advances in Water Resources, v.159, 14 p.

Warner, D. L., and Syed, T., 1986, Confining layer study-supplemental report, prepared for U.S. EPA Region V, Chicago, Illinois.

Warner, D. L., 1988, Abandoned oil and gas industry wells and their environmental implications: prepared for the American Petroleum Institute.

Wattenbarger, R. A., 1999, Formation Compressibility: Report for DuPont

Yale, D. P., Nabor, G. W., Russell, J. A., Pham, H. D., and Yousef, M., 1993, Application of variable formation compressibility for improved reservoir analysis: Society of Petroleum Engineers, Society Petroleum Engineers Paper 26647, Houston, Texas, p. 435-450.

Yamamotoa, H. and Doughty C.B., 2011, Investigation of Gridding Effects for Numerical Simulations of CO2 Geologic Sequestration, International Journal of Greenhouse Gas Control, Volume 5, Issue 4, pp 975-985